5-4-2021

Toxicological Characterization of Traffic-related Air Pollution in Five Distinct Atlanta Locations

Haris Bejdic

Toxicological Characterization of Traffic-Related Air Pollution in Five Distinct Atlanta Locations

By

Haris Bejdic

May 2, 2021

ABSTRACT

Traffic-related air pollution (TRAP) affects approximately 45 million individuals who live within 300 feet of a major highway, resulting in adverse respiratory and cardiovascular outcomes (e.g., asthma, inflammation). Recent studies indicate that green infrastructure reduces aerosol concentrations and potentially limits TRAP-related toxicity. We hypothesized that green infrastructure might mitigate reactive oxygen species (ROS) generation, oxidative stress, cytokine secretion, and potential inflammation and injury in human primary small airway epithelial cells (SAEC) associated with similar respiratory pathologies, including asthma. TRAP was monitored at five Atlanta locations (S1: green barrier; S2: no barrier; S3: combination barrier; S4: no barrier; S5: green barrier) next to and behind barriers using continuous instrumentation, and sampled particulate matter (PM) was collected on pre-weighed polytetrafluoroethylene (PTFE) filters. The collected PM was extracted and prepared for toxicological assessments, including CellROX®, total glutathione (GSH), and MTS assays, which measured ROS production, oxidative stress, and cellular viability, respectively, using SAEC following a 48-hour exposure period. Additionally, the Human Cytokine Array Proinflammatory Focused 15-plex (HDF15) was used to evaluate the secretion of pro-inflammatory cytokines, such as granulocyte-macrophage colony-stimulating factor (GM-CSF), interleukin-8 (IL-8), monocyte chemoattractant protein-1 (MCP-1), and tumor necrosis factor-alpha (TNF-α). Preliminary *in vitro* toxicological analyses revealed that sites with green barriers (e.g., S1, S5) decreased TRAP-induced impacts on oxidative stress and cytokine secretion in SAEC. However, there was no reduction in cell viability following PM exposures. Additionally, a site with a combination barrier (e.g., S3) decreased GM-CSF, IL-8, and TNF-α cytokine secretion in SAEC. TRAP exposures may elicit harmful pulmonary mechanisms, including inflammation and oxidative stress in lung epithelial cells over time. This work suggests green barriers may influence the biological activity of PM. In sum, green barriers may play a role in mitigating TRAP-mediated respiratory health effects.

Toxicological Characterization of Traffic-Related Air Pollution in Five Distinct Atlanta Locations

By

Haris Bejdic

Bachelor of Science, University of Georgia

May 2, 2021

A Thesis Submitted to the Graduate Faculty
of Georgia State University in Partial Fulfillment
of the
Requirements for the Degree

MASTER OF PUBLIC HEALTH

ATLANTA, GEORGIA
30303

APPROVAL PAGE

Toxicological Characterization of Traffic-Related Air Pollution in Five Distinct Atlanta Locations

By

Haris Bejdic

Approved:

Dr. Christa Watson-Wright
Committee Chair

Dr. Christina Fuller
Committee Member

Dr. Ruiyan Luo
Committee Member

Dr. Katherine Masyn
Department Chair

May 2, 2021
Date

ACKNOWLEDGEMENTS

We want to thank the National Institute of Environmental Health Sciences for providing the opportunity to conduct this research through their funding (grant number: ES02925201A1). I also want to extend my thanks and appreciation to my mentor and committee chair, Dr. Christa Wright, for providing me with this opportunity, giving me guidance and direction, and providing me with patient advice. I also want to thank my other committee members, Dr. Christina Fuller and Dr. Ruiyan Luo, for agreeing to take this journey with me. Lastly, I want to thank my family and friends for being patient throughout this process, always supporting me, and giving me positive, kind feedback throughout my journey. I am forever grateful for everyone who played a role in my academic accomplishments.

AUTHOR'S STATEMENT

In presenting this thesis as a partial fulfillment of the requirements for an advanced degree from Georgia State University, I agree that the library of Georgia State University shall make it available for inspection and circulation in accordance with its regulations governing materials of this type. I agree that permission to quote, to copy from, or to publish this thesis may be granted by the author or, in his/her absence, by the professor under whose direction it was written, or in his/her absence, by the Associate Dean, School of Public Health. Such quoting, copying, or publishing must be solely for scholarly purposes and will not involve potential financial gain. It is understood that any copying from or publication of this thesis which involves potential financial gain will not be allowed without written permission of the author.

Haris Bejdic
Signature of Author

TABLE OF CONTENTS

LIST OF TABLES

LIST OF FIGURES

1. INTRODUCTION

Air pollution refers to the release of pollutants into the environment that harms human health, resulting in adverse respiratory, cardiovascular, and biological outcomes. The U.S. Environmental Protection Agency (EPA) continuously monitors and regulates air quality trends using criteria pollutants, including carbon monoxide (CO), lead, nitrogen dioxide (NO_2), ozone, particulate matter ($PM_{2.5}$ and PM_{10}), and sulfur dioxide (SO_2). Traffic-related air pollution (TRAP) refers to air pollution derived from motor vehicle emissions following fossil fuel combustion. In other words, TRAP encompasses combustion emissions (contributed primarily by on-road diesel and gasoline vehicles), secondary pollutants formed in the atmosphere, such as inorganic and organic molecules, and non-combustion emissions, including but not limited to road dust and brake/tire wear (Matz et al., 2019). TRAP exposures have been implicated in several adverse health outcomes, including premature mortality (Jerrett et al., 2009), cardiovascular outcomes (Brook et al., 2010; Cesaroni et al., 2014; Lanki et al., 2006; Link & Dockery, 2010), cerebrovascular outcomes (Stafoggia et al., 2014), respiratory outcomes (Gasana et al., 2012; Gehring et al., 2010; Lindgren et al., 2009; MacIntyre et al., 2014), reproductive outcomes (Brauer et al., 2008; Yorifuji et al., 2016), and neurological as well as cognitive disorders (Power et al., 2016; Raz et al., 2015).

Vulnerable subpopulations, including but not limited to young children (Clark et al., 2010; Clifford et al., 2018; Gasana et al., 2012; McConnell et al., 2010), the elderly (Delphino et al., 2014), racial/ethnic groups (Apelberg, Buckley, & White, 2005; Park & Kwan, 2020; Tian, Xue, & Barzyk, 2012), and socioeconomically deprived individuals (Apelberg, Buckley, & White, 2005; Chi et al., 2016; O'Neill et al., 2003; Tian, Xue, & Barzyk, 2012) across the U.S., are susceptible to TRAP exposures (Hooper & Kaufman, 2018; Makri & Stilianakis, 2008). These

subpopulations are exposed to TRAP due to their proximity to major highways/roadways as well as intersections of major roads and certain underlying diseases, such as asthma (Clark et al., 2010; Clifford et al., 2018; Gasana et al., 2012; McConnell et al., 2010), hypertension (Delphino et al., 2014; Brook et al., 2009; Kaufman et al., 2016), and lung cancer (Apelberg, Buckley, & White, 2005; Churg et al., 2003; Health Effects Institute, 2010). Acute and chronic exposures to PM components of TRAP, specifically ultrafine particles (UFPs), and their associated toxicological properties, however, remain to be thoroughly investigated. Potential interventions and strategies that may reduce TRAP exposures for susceptible subpopulations include investing in green infrastructure (i.e., trees, vegetation; Amorim et al., 2013; Brugge et al., 2015), investing in biking and walking trails in neighborhoods within urban cities (Brugge et al., 2015) and developing alternate public transportation options appropriate for all individuals (Xia et al., 2015).

We aim to address the following experimental questions: 1) What is the toxicological impact of traffic-related UFP concentrations on the respiratory system? 2) What TRAP properties mediate adverse cellular outcomes? 3) Can green infrastructure help mitigate or reduce these observed cellular effects? We hypothesize that green infrastructure may mitigate ROS generation, oxidative stress, cytokine secretion, and potential inflammation and injury in human primary small airway epithelial cells (SAEC) associated with respiratory pathologies such as asthma. An *in vitro* dose-response analysis using cellular bioassays, including the CellROX®, total glutathione (GSH), and MTS assays, was performed to measure ROS production, oxidative stress, and cellular viability, respectively. The Human Cytokine Array Pro-inflammatory Focused 15-plex (HDF15) from Eve Technologies (Alberta, Canada) was used to test for the following cytokines: granulocyte-macrophage colony-stimulating factor (GM-CSF), interferon gamma (IFNγ),

interleukin-1β (IL-1β), IL-1ra, IL-2, IL-3, IL-4, IL-5, IL-6, IL-8, IL-10, IL-12(p40), IL-12(p70), monocyte chemoattractant protein-1 (MCP-1), and tumor necrosis factor-alpha (TNF-α). Lastly, a one-way ANOVA analysis involving Tukey's post-hoc test and descriptive statistics were utilized to relate sampling location and UFP concentrations to all cellular outcomes, such as ROS generation, subsequent oxidative stress, antioxidant capacity, cellular viability, and cytokine secretion in SAEC.

2. REVIEW OF THE LITERATURE

2.1 Historical Overview of Air Pollution in the U.S.

Substandard air quality contributes to adverse health outcomes, leading to increased morbidity, mortality, and global disease burden (Samek, 2016). Since the Clean Air Act passage in the year 1970, air quality in the U.S. has significantly improved, as shown by the reduction of concentrations among all criteria air pollutants (since the 2000s for $PM_{2.5}$; U.S. EPA, 2020). Among the several emissions sources (e.g., stationary fuel combustion, industrial and other processes), highway vehicles emit mainly CO and NO_2, followed by volatile organic compounds, $PM_{2.5}$, PM_{10}, and SO_2 being the lowest concentration (Sohrabi, Zietsman, & Khreis, 2020; U.S. EPA, 2019; U.S. EPA 2020).

Air-pollutant concentrations are not distributed equally across the U.S. or within cities. Factors that influence air quality differences include urban and rural settings, socioeconomic status (i.e., lower-income versus higher-income), and race/ethnicity. Ingram and Franco (2014) examined the 2013 urban-rural county categorization scheme, ranging from metropolitan to nonmetropolitan counties. Metropolitan ("metro") counties include large central metro counties (consisting of 1,000,000 or more individuals), large fringe metro counties (consisting of 1,000,000 or more individuals that do not qualify as large central metro counties), medium metro counties (consisting of 250,000 to 999,999 individuals), and small metro counties (consisting of less than 250,000 individuals). Nonmetro counties include micropolitan counties (consisting of 10,000 to 49,999 individuals) and noncore counties (i.e., nonmetro counties that do not qualify as micropolitan counties). Nearly 31% of U.S. citizens live in urban counties (Strosnider et al., 2017). In contrast, about 6% of U.S. citizens live in rural counties or county-equivalents (i.e., nonmetro counties

containing fewer than 10,000 people; Strosnider et al., 2017). Two hundred eighty-six (286) counties transitioned to a different county category assignment (i.e.., from a less urban metro county to a more urban metro one, from a nonmetro county to a metro one) between 2006 and 2013 (Ingram & Franco, 2014). People residing in a rural county or county-equivalent, on average, experienced 8.87 micrograms per cubic meter ($\mu g/m^3$) in $PM_{2.5}$ concentrations compared to 11.15 $\mu g/m^3$ in urban counties between 2008 and 2012 (Strosnider et al., 2017).

The United Nations estimates that 68% of the world's population will reside in urban settings by 2050 (2014). The U.S. Bureau of Transportation Statistics reported a 1% increase in the total number of registered highway vehicles (roughly 2,900,000 vehicles) between 2018 and 2019 (n.d.). Between 2018 and 2019, the nation's population grew by approximately 1,500,000 people (0.5% increase; U.S. Census Bureau, 2019). States depend on census information to distribute revenue from taxes to undergo significant local-road expansions and renovations (America Counts Staff, 2019) to accommodate increased vehicular activity and alleviate traffic. Construction projects like these, however, generate increased air pollutant concentrations since vehicular activity remains relatively the same or increases following road expansion (Font et al., 2014).

2.1.1 Disparities in Pollution Concentrations

Jorgenson and colleagues (2020) reviewed the power, proximity, and physiology principles, suggesting that vulnerable populations' exposure to ambient air pollution increases as income inequality increases in terms of economic or political influence, geographical space, or underlying physiological conditions, respectively (Hill et al., 2019). The three-way interaction

between power, proximity, and physiology occurs at an amplified rate in states exhibiting higher income-inequality levels and states with larger minority populations. Blacks and Hispanics residing in urban settings typically live in more polluted cities and neighborhoods within those cities than their Asian and White counterparts (Ash & Fetter, 2004; Gray, Edwards, & Miranda, 2013). Racial/ethnic disparities highlighted by geographic location (i.e., urban versus rural or proximity to a major highway/roadway) and income inequality reveal differences in air pollution exposure rates. Tessum and colleagues (2019) analyzed how primarily industrial fuel combustion, followed by recreational and residential fuel combustion (e.g., operating recreational vehicles, barbecuing), negatively impact Blacks and Hispanics compared to non-Hispanic Whites. After adjusting for race/ethnicity to match other racial/ethnic groups without modifying consumption rates, Blacks were exposed to at least two times the $PM_{2.5}$ concentration experienced by the overall population (Tessum et al., 2019).

Compared to their non-Hispanic White counterparts, Blacks and Hispanics contribute little to the average $PM_{2.5}$ pollution levels yet experience at least 21% higher exposure (for Blacks) and 12% higher exposure (for Hispanics; Tessum et al., 2019). According to Tessum and colleagues, total exposure emissions include but are not limited to road dust, residential gas and wood combustion, construction, and agriculture. Pollution inequities, or the differences between the environmental health damage caused by a racial-ethnic group and the damage that group experiences, via differences in consumption trends highlight the racial disparities endured by Blacks and Hispanics compared to their non-Hispanic White counterparts. After normalizing the magnitude effect (i.e., the total amount of consumption), however, Blacks and Hispanics are exposed to increased $PM_{2.5}$ levels than non-Hispanic Whites (Tessum et al., 2019).

2.2 Traffic-Related Air Pollution and Mitigation Measures

Approximately 45 million individuals live, work, and attend school within 300 feet of major roadways (U.S. EPA, 2020), resulting in adverse health effects (e.g., respiratory, cardiovascular, reproductive) due to TRAP exposures (Nuvolone et al., 2011). Depending on a location's infrastructure and meteorology, TRAP concentrations can vary spatially and temporally (Cheng et al., 2019). Due to the inadequate information regarding traffic-source contribution to TRAP and the limited ability to collect and monitor air pollutants, however, it proves challenging to measure spatial and temporal variations in TRAP accurately (Batterman, Ganguly, & Harbin, 2015; Health Effects Institute, 2010; Wang et al., 2013). Generally, the summer months in the U.S. (June, July, and August) are typically dominated by secondary aerosols formed through gas-to-particle conversion compared to the winter months (December, January, and February), which are usually dominated by primary aerosols introduced directly into the air (Cheng et al., 2019). Current evidence shows that increased TRAP levels persist near major highways/roadways and intersections of major roads. Similarly, spatial and temporal variations in TRAP occur due to distinct urban structures and traffic modes that lead to different pollutant distribution patterns over time (Wang et al., 2013).

Enacting emission reduction policies, limiting TRAP exposures, and installing porous (e.g., trees, vegetation) and solid barriers (e.g., noise walls, low-boundary walls) may present as viable options to mitigate TRAP exposures (Gallagher et al., 2015). After introducing TRAP reduction methods, such as motor vehicle emission standards (Lurmann, Avol, & Gilliland, 2015), increasing active transportation usage (e.g., cycling) to minimize vehicular activity (Carlsten et al.,

2020; Raza et al., 2018), shortening the time spent outside near major highways/roadways (Carlsten et al., 2020; Laeremans et al., 2018), and investing in green infrastructure (Baldauf, 2016; Gallagher et al., 2015; Hewitt, Ashworth, & MacKenzie, 2020; Litschke & Kuttler, 2008), air pollutant concentrations have been shown to decrease over time.

Lurmann, Avol, and Gilliland examined motor vehicle emission standards in California by measuring ambient criteria-pollutant concentrations (e.g., ozone, NO_2, $PM_{2.5}$, PM_{10}) between 1993 and 2012 and obtaining emission policy information from a regulatory database (2015). The researchers discovered that criteria-pollutant concentrations significantly decreased (i.e., an approximately 3% decrease for ambient $PM_{2.5}$ concentrations) due to declines in motor vehicle emissions via reduction standards (Lurmann, Avol, & Gilliland, 2015). Raza and colleagues performed a risk assessment to compare the relative risks (i.e., the ratio of the risks for an event for the exposure group to the risks for an event for the non-exposure group) from previous studies that examined shifts in transportation modes, such as the transition from motorized travel to cycling (2018). While the researchers only examined eighteen studies in their review, they determined that the general population's health benefits and the commuters' health risks undervalue the effect of vehicle exhaust exposure even though car users experienced 1.16 to 1.6 times higher $PM_{2.5}$ concentrations than cyclists (Raza et al., 2018).

Hewitt, Ashworth, and MacKenzie reviewed how trees and other vegetation barriers (i.e., green barriers) can protect individuals by creating natural shields against TRAP or redirecting airflow above the green barriers, suggesting how developing green spaces can effectively reduce TRAP levels to improve urban air quality ultimately (2020). Gallagher and colleagues noted that

urban infrastructure (i.e., barrier/street geometry and roadway layout) plays a significant role in mitigating air pollution (2015). Combining porous and solid barriers to optimize the effect of reducing air pollution in urban locations, particularly near major highways/roadways, can offer a quality solution compared to either installed barrier alone (Gallagher et al., 2015).

Jayasooriya and colleagues explored the impact green infrastructure, specifically trees, green roofs, green walls, and a combination of any of the previously mentioned scenarios (i.e., trees and green roofs, trees and green walls, green roofs and green walls), has on urban air quality and other factors in several cities, including but not limited to Atlanta, GA, New York, NY, Baltimore, MA, and Philadelphia, PA (2017). Besides the environmental factors, such as annual pollutant removal, other factors included economic costs and savings as well as social livability improvement (Jayasooriya et al., 2017). Two scenarios – trees and green roofs and trees and green walls – provided increased protection against TRAP, particularly $PM_{2.5}$ and PM_{10}, compared to any other presented scenario alone (Jayasooriya et al., 2017). Trees and green roofs as well as green roofs and green walls resulted in increased annual building energy savings and lowered capital costs and annual operation and maintenance costs (Jayasooriya et al., 2017). Trees and green roofs also improved social livability, followed closely by trees and green walls (Jayasooriya et al., 2017).

2.3 U.S. Air Quality Regulations

The University of Washington Institute for Health Metrics and Evaluation reported that PM is accountable for nearly 60% of deaths from environmental causes (2016). PM contains minuscule solids or liquid droplets that individuals can inhale, leading to adverse health outcomes.

PM particles, typically formed by chemical reactions with atmospheric traffic-related air pollutants (also known as secondary pollutants), can differ in aerodynamic diameter: coarse PM_{10} (particles that measure less than 10 micrometers in diameter), fine $PM_{2.5}$ (particles that measure less than 2.5 micrometers in diameter), and $PM_{0.1}$ (particles that measure less than 0.1 micrometers in diameter). The PM size determines where particles will accumulate in the human body (i.e., the upper respiratory tract [URT] for PM_{10}, the tracheobronchial regions for $PM_{2.5}$, the distal alveolar regions for $PM_{0.1}$). The URT includes the nose and mouth. The tracheobronchial regions refer to the airway between the trachea and terminal bronchioles in the lungs. Distal alveolar regions are where gas exchange occurs that cross the blood barrier into other organs throughout the body. Particle diameter negatively correlates with associated toxicity and lung deposition (i.e., increased toxicity occurs following exposure to smaller PM sizes, and the size dictates where in the body the particles will deposit). PM_{10} is filtered in the proximal airway (i.e., the URT), which may irritate the skin and mucosa. $PM_{2.5}$ can reach the peripheral airway (i.e., the tracheobronchial regions) but cannot enter the systemic circulation. Due to its large surface area, $PM_{0.1}$ can adsorb toxic chemicals, including elemental and organic carbon, water-soluble ions, and other trace elements (e.g., polycyclic aromatic hydrocarbons [PAHs]), on its surface, which may enter the systemic circulation (Chen et al., 2010; Haghani et al., 2020; Kwon, Ryu, & Carlsten, 2020). Desorption of these toxic chemicals and $PM_{0.1}$ cellular interactions can result in a dual exposure, which may exacerbate or increase adverse health effects (Chen et al., 2010; Haghani et al., 2020; Kwon, Ryu, & Carlsten, 2020).

$PM_{0.1}$ particles (also known as UFPs) have been linked to unfavorable respiratory effects, including but not limited to asthma, chronic obstructive pulmonary disease (COPD), emphysema,

and lung cancer (Clifford et al., 2018; Health Effects Institute, 2010). While researchers continuously assess how $PM_{2.5}$ and PM_{10} adversely affect human health, limited knowledge exists on how $PM_{0.1}$ leads to decreased respiratory function since no standards are present for PM smaller than 2.5 micrometers in diameter. It is known, however, that UFPs contain unusually high amounts of elemental and organic carbon in the form of black carbon (BC) as well as PAHs, carbonyl compounds, n-alkanes, organic acids, and heterocyclic compounds, respectively, among other chemicals and molecules (Chen et al., 2010; Kwon, Ryu, & Carlsten, 2020). Previous studies have reported the adverse health effects caused by elemental and organic carbon (Kelly & Fussell, 2012; Ostro et al., 2008; Ostro et al., 2009).

According to the Clean Air Act, a U.S. federal law designed to protect human health and the environment from air pollution effects, the EPA must regulate pollutant emissions that harm public health and welfare. To do this, the EPA continuously updates primary and secondary National Ambient Air Quality Standards (NAAQS) for criteria pollutants (2016). Primary standards establish limits to protect vulnerable populations' health, whereas secondary standards set limits to protect the environment. Currently, primary and secondary standards for $PM_{2.5}$ and PM_{10} require annual average standards (primary standard for $PM_{2.5}$: annual mean, averaged over three years, of 12.0 $\mu g/m^3$; secondary standard for $PM_{2.5}$: annual mean, averaged over three years, 15.0 $\mu g/m^3$) and daily standards (primary and secondary standards for $PM_{2.5}$: 98^{th} percentile, averaged over three years, of 35 $\mu g/m^3$; primary and secondary standards for PM_{10}: not to exceed 150 $\mu g/m^3$ more than once per year on average over three years).

$PM_{0.1}$ and $PM_{2.5}$ concentrate near highways, dependent on roadway layout, traffic volume, vehicle type, and atmospheric conditions. Kuwayama, Ruehl, and Kleeman observed five different conditions in which $PM_{0.1}$ mass concentrations increased in downtown Sacramento, California: old diesel engines, residential wood smoke, rails, regional traffic (i.e., gasoline and diesel engines), and brake wear/paved road dust (2013). In addition to measuring $PM_{0.1}$ mass, $PM_{0.1}$ composition was also determined to pinpoint which chemicals (i.e., elemental and organic carbon, sulfur, and other trace elements) exhibited high levels within the collected $PM_{0.1}$ (Kuwayama, Ruehl, & Kleeman, 2013). Chemicals adsorbed onto UFP surfaces pose a serious health risk for individuals inhaling them. This study further supports the need for emissions standards and other practical mitigation efforts since older (diesel) engines, on average, contributed to approximately 25% of total $PM_{0.1}$ concentrations (Kuwayama, Ruehl, & Kleeman, 2013). Previous studies have suggested vehicular activity contributes to 20% of $PM_{2.5}$ variation (i.e., changes in concentration, spatiotemporal changes; Milando, Huang, & Batterman, 2016; Morishita et al., 2006).

Historically, PM monitoring and sampling have been used to investigate TRAP exposures, determine the air quality in a country or region, and assess several mitigation strategies' effectiveness. Standard PM monitoring methods include but are not limited to continuous mass monitoring, such as opacity monitors, light-scattering technologies, and tapered-element oscillating microbalance (TEOM; Wilson et al., 2002). The objective of continuous mass monitoring includes measuring real-time PM mass found in ambient air (Solomon & Sioutas, 2008). Opacity monitors, such as microaethalometers which measure BC, quantify the extent to which PM reduces light transmission (Eiseman, 1998). Microaethalometers are easy to operate, only requiring Teflon™ coated glass fiber filter media. Among other optical PM monitoring

methods, however, opacity devices are the least sensitive due to a minor measurable change in light transmission in a considerable amount of emission (Eiseman, 1998). Light-scattering technologies account for PM composition, size distribution, and volume to observe particle loading by measuring the light reflected from the particles' surfaces forwards, backwards, and sideways. Forward-, backward-, and side-scattering technologies range in sensitivity from worst to best, respectively. However, these technologies are expensive, and all scattering methods require calibrations to function correctly. TEOM directly measures PM mass by relating it to the mass's frequency output, which exhibits a negative correlation (i.e., as the mass increases, the frequency output decreases and vice versa). While TEOM is sensitive to all particles, it is challenging to control the humidity and temperature while using this method.

Standard PM sampling methods, such as the gravimetric (weighing) method using filters, measure its concentration. In the gravimetric method, particles agglomerate onto a pre-weighed filter, and the filter is reweighed following collection. This method's advantage includes the ability to chemically analyze the collected particles (Nussbaumer et al., 2008; Whalley & Zandi, 2016). However, the gravimetric method does not offer data outside of the period in which the filter was stationed. Additionally, this method requires accurate weighing, and an imprecise weighing procedure can negatively influence measurements (i.e., measurements can vary between weighings). PM collected on filters can be extracted into an aqueous solution using methanol (MeOH), water, dichloromethane (DCM), and dimethylsulfoxide (DMSO; Roper et al., 2020). Water and MeOH yield the highest concentrations compared to other solvents (Roper et al., 2020).

2.4 TRAP-Associated Adverse Health Outcomes, Cellular Responses, and Biomarkers

TRAP exposures have been linked to adverse respiratory (Ostro et al., 2009; Sydbom et al., 2001; Vimercati, 2011), cardiovascular (Brook et al., 2004; Ostro et al., 2008), reproductive (Brauer et al., 2008), and biological/genetic (De Prins et al., 2013; Ji & Khurana Hershey, 2013) outcomes. Harmful respiratory outcomes resulting from TRAP exposures can include but are not limited to asthma (Ostro et al., 2009; Clifford et al., 2018), bronchitis (Lindgren et al., 2009), COPD (Andersen et al., 2011; Ling & van Eeden, 2009), emphysema (Wang et al., 2019), and lung cancer (Beelen et al., 2008; Chen et al., 2015). Susceptible subpopulations, including but not limited to young children, the elderly, and specific racial/ethnic groups, are more at-risk for TRAP-associated adverse respiratory effects and outcomes due to age and related physiological differences in inhalation rates (U.S. EPA, 2011), underdeveloped immune and respiratory systems mainly in young children (Bowatte et al., 2015; Deng et al., 2016), and existing comorbidities primarily in the elderly (de Hartog et al., 2003; Delphino et al., 2014).

TRAP exposures have been known to promote reactive oxygen species (ROS) generation (Lakey et al., 2016; Venkatachari & Hopke, 2008; Verma et al., 2015), increase oxidative stress (Bräuner et al., 2007; Møller & Loft, 2010; Risom, Møller, & Loft, 2005), decrease antioxidant capacity (Cosselman et al., 2020) and cellular viability (Li et al., 2017; Wu et al., 2017), as well as induce cytokine secretion (Boland et al., 2000; Sawyer et al., 2010; Silbajoris et al., 2011). ROS, including but not limited to superoxide, hydrogen peroxide (H_2O_2), and hydroxyl radical, refer to oxygen-containing reactive species. ROS form endogenously due to underlying chemical reactions during mitochondrial oxidative phosphorylation or exogenously via interactions with foreign compounds (i.e., xenobiotics) entering the cell (Ray, Huang, & Tsuji, 2012). Overproduction of ROS can affect protein function by damaging RNA, mutate DNA to lead to cellular dysfunction,

deplete ATP reserves, and inhibit apoptosis (i.e., programmed cell death) by directly oxidizing relevant compounds and molecules (Risom, Møller, & Loft, 2005; Rosanna & Salvatore, 2012). ROS have also been linked to cancer initiation and development (Cichon & Radisky, 2014). Oxidative stress occurs when excess ROS or oxidants overwhelm a cell's antioxidative defenses (Ray, Huang, & Tsuji, 2012), potentially leading to cellular inflammation and injury. The cell's resulting antioxidant capacity, or its ability to protect against the oxidative damage done to it, declines. When toxic insults occur, the cell cannot protect itself against incoming damage, resulting in a higher number of damaged or dying cells within a population (i.e., diminished cell viability). Cellular viability refers to the number of healthy cells in a sample.

Pro-inflammatory cytokines and chemokines that mediate the cell's innate immunological response to toxic insults can include but are not limited to granulocyte-macrophage colony-stimulating factor (GM-CSF), interleukin-8 (IL-8), monocyte chemoattractant protein-1 (MCP-1), and tumor necrosis factor-alpha (TNF-α), which are mainly produced by activated macrophages and monocytes (Zhang & An, 2007). GM-CSF is a monomeric glycoprotein secreted by macrophages and T helper cells that induces the recruitment and migration of cells to inflammation sites, promotes survival of target cells, and stimulates granulocyte- and macrophage-regeneration (Zhang & An, 2007). IL-8 is a chemotactic factor that recruits neutrophils, basophils, and T-cells to inflammation sites and can be secreted by several structural and immune cells, including bronchial epithelial cells, macrophages, and smooth muscle cells (Zhang & An, 2007). MCP-1 (also known as CCL2) is a chemotactic factor that recruits monocytes to inflammation sites and is produced by various cell types following induction by oxidative stress, cytokines, or growth factors (Deshmane et al., 2009). Macrophages and monocytes produce TNF-α during the inflammatory

process, which recruits other immune cells to the damaged site via signaling and can elicit apoptosis and necrosis (i.e., localized death of living tissue; Zhang & An, 2007).

Typical *in vitro* bioassays detecting ROS production can include but are not limited to the CellROX® and ROS-Glo™ H_2O_2 assays that use stains and luminescence, respectively, to examine the effects of oxidative stress on exposed cells. The CellROX® assay (Invitrogen, California, U.S.) can employ the Oxidative Stress Orange Reagent, a cell-permanent dye that exhibits bright orange fluorescence upon oxidation by ROS. In contrast, the ROS-Glo™ H_2O_2 assay (Promega, Wisconsin, U.S.) utilizes an H_2O_2 substrate that reacts with a luciferin precursor to produce luciferin that emits a light signal proportional to the level of H_2O_2. Other methodologies detecting ROS production can include the comet and DTT assays (Jantzen et al., 2012; Jiang et al., 2019). A commonly-used *in vitro* bioassay detecting oxidative stress can include but is not limited to the GSH/GSSG-Glo™ Assay (Promega, Wisconsin, U.S.) that detects and quantifies the antioxidant glutathione (GSH), a relevant component in cellular metabolism, and other related compounds (e.g., glutathione disulfide [GSSG]) in exposed cells. Another methodology detecting oxidative stress includes the antioxidant depletion assay (Crobeddu et al., 2020). Standard *in vitro* bioassays assessing cellular viability can include but are not limited to the MTS and MTT assays (Promega, Wisconsin, U.S.), which measure metabolic activity by introducing a soluble tetrazolium salt to the cells and observing whether or not it is metabolized. Another method assessing cellular viability includes the LDH (lactate dehydrogenase) assay, which determines irreversible cell death by examining whether or not membrane damage has occurred depending on how much cytoplasmic lactate has been released from damaged or dying cells (Thomson et al., 2015).

3. METHODS AND PROCEDURES

3.1 TRAP Sampling Campaign

The data sampling collection campaign was designed to measure relative UFP numbers, particle-size distributions, and total mass concentrations during peak traffic periods between July and September 2020. Daily sampling occurred at times with increased traffic pollutant emissions in the morning and afternoon (from 7 am to 3 pm). Each sampling day began the same, with instrumentation set-up occurring first. Continuous instruments, including condensation particle counters (CPC model 3007, TSI Incorporated, Minnesota, U.S.), microaethalometers (microaethalometer model AE51, AethLabs, California, U.S.), microsensors that used a Plantower $PM_{2.5}$ PMS3003 particle counter (Duke University, North Carolina, U.S.), a NanoScan Scanning Mobility Particle Sizer (NanoScan SMPS model 3910), an Optical Particle Sizer (OPS model 3330, TSI Incorporated, Minnesota, U.S.), Vantage Pro 2 or Vantage Vue weather station (Davis Instruments, California, U.S.) as well as one Hobo weather station (Onset, Massachusetts, U.S.) were set up near selected green barriers and roadways (Figures 1, 2). Each site consisted of two sampling locations at least 20 meters (m) apart when continuous and integrated sampling took place. Weather stations were placed on-site to collect data on wind speed, wind direction, temperature, and relative humidity (Figure 2).

At the start and end of each sampling day, the CPCs, microaethalometers, and microsensors were turned on simultaneously to initiate side-by-side sampling, ensuring that the continuous instruments reported the same data points. Unlike the CPCs, microaethalometers, and microsensors, the NanoScan SMPS and OPS instruments were not used during side-by-side sampling in the morning and afternoon since only one instrument was used. Instrumentation was

initially placed on a mobile cart for side-by-side sampling, and identical instruments were later placed at both roadway and barrier locations. For those sites with no barriers (S2 and S4), instruments were placed at least 20 m apart. Any issues with instrumentation (e.g., depleted batteries) or suspected reasons for unusually high readings (e.g., vehicular idling) were documented on a log sheet throughout the sampling day. Other pertinent information, such as sample IDs, instrumentation start and end times, and initial and ending flow rates for the cascade particle impactors constructed in our laboratory (Figure 2) used to collect PM on polytetrafluoroethylene (PTFE) filters, was also recorded. A total of twelve sampling days were completed at five distinct Atlanta locations: S1-S5 (Figure 3; Tables 1, 2). Green barriers were present at S1 and S5, and a combination barrier (i.e., trees, sound wall) was present at S3. No barriers were present at S2 and S4. In the "Road versus Barrier" column of Tables 1 and 2, "NA (Front-Road/Side-Road)" indicates where the filter was collected since S2 and S4 did not contain barriers (i.e., not applicable). Site locations varied by roadway layout and traffic volume.

$PM_{1.0}$ mass, which included particles from the ultrafine range up to 1.0 micrometers in diameter, was collected on four pre-weighed PTFE filters using cascade impactors during each sampling day. After setting up two cascade impactors (one at the green barrier and the other at the roadway or, if no barrier was present, both at the roadway 200 m apart) that each collected PM mass on two separate filters, flow rates were measured, confirming a rate of 30 Liters/minute. Following sample collection, filters were transported back to the laboratory and left in a desiccator to equilibrate for 24 hours to a temperature of 25°C and 15% relative humidity. Filters with any leftover static charge were dissipated using a U-electrode (Mettler Toledo model 11140161) and then weighed with a Mettler Toledo microbalance (model XS3DU) following Georgia State

University (GSU) approved safety measures and protocols. Each sample was weighed at least two times, ensuring that the weight did not differ more than 5 μg between weights. Laboratory blanks and field blanks (at least one filter for each site) were weighed using the same protocol. Laboratory blanks were left in the desiccator during the sampling campaign. Field blanks were left in a box used to transport filters during sampling.

3.2 PTFE Filter Extraction

Each PTFE filter was extracted using 5 milliliters (mL) of 75% MeOH. 75% MeOH was prepared in different amounts using MeOH (Sigma Aldrich, Missouri, U.S.) and deionized water (di H_2O). Filters were first placed upside down inside a plastic beaker (with the collected samples facing the bottom of the plastic beaker). 5 mL of 75% MeOH was added aseptically using a serological pipette (following standard GSU safety measures and protocols), ensuring that the MeOH completely covered each PTFE filter. Parafilm and aluminum foil coverings were then placed onto the plastic beakers. Each PTFE filter was sonicated separately at 45% amplitude for four minutes in an ice-water bath, continuously refilling the cup sonicator (Branson Ultrasonics Sonifier S-250D, ThermoFisher, Massachusetts, U.S.) with ice as needed. Following cup sonication, each sample was then transferred to a plastic 15 mL conical tube to be eventually frozen at -80°C until needed later for toxicological analyses. Before freezing samples, they were vacufuged at 60°C using the Eppendorf Vacufuge Plus (Eppendorf, Massachusetts, U.S.) for approximately three hours (time spent vacufuging ranged from two hours to six hours) down to 5 microliters (μL) of sample to eliminate any residual MeOH. PTFE filters were weighed again at least twice after allowing them to dry in the desiccator for one day to determine the total mass extracted (i.e., initial concentration). Extraction efficiencies (in %; Table 1) were calculated by

subtracting the average post-extraction weight from the average post-collection weight, dividing the minuend by the total particle mass collected (Table 1), and multiplying the quotient by 100%. Extracted and vacufuged samples were then placed into a -80°C freezer until experimentation. On experimentation days, samples were taken out of the freezer and left to thaw at room temperature. After each sample was thawed, they were sonicated in batches of five to seven samples at 45% amplitude for four minutes to homogenize the sample mixtures in preparation for dilutions.

3.3 Multiple-Path Particle Dosimetry Model Dose and Dilution Calculations

The Multiple-Path Particle Dosimetry Model (MPPD version 3.04) was used to determine the low (4 μg/mL) and high (20 μg/mL) doses for each sample. Assuming that individuals spend nearly 0.86 hours per day for five days each week for 52 weeks commuting to work and being stuck in traffic (Knoblauch, 2019) and engaging in recreational activities outside (U.S. Bureau of Labor Statistics, 2020), this data was used to calculate the total amount of PM ($\mu g/cm^2$) reaching the pulmonary region per alveolar area in an adult. Low concentrations (4 μg/mL) represent individuals going to work or spending time outside for 0.86 hours per day for five days each week for one year, whereas high concentrations (20 μg/mL) represent individuals going to work or spending time outside for 0.86 hours per day for five days each week for five years.

The total amount of PM ($\mu g/cm^2$) reaching the pulmonary region was divided by 70 m^2 (Dunhill, 1962) to obtain the mass of PM per alveolar area used to calculate the doses utilized in the toxicological experiments. The quotient was then multiplied by the total surface area of one well (0.33 cm^2) in a 96-well plate used for growing the SAEC. For example, the total amount of PM reaching the pulmonary region, 991 $\mu g/cm^2$, was divided by 70 m^2, and the quotient was

multiplied by 0.33 cm^2 to obtain a final product of 0.00046719 $\mu g \cdot cm^2$ (i.e., approximately 0.0004 μg) of PM in a single well. After determining the deposited mass for the pulmonary region, a dose-response assessment was conducted using 0.0004 μg/mL (as a starting dose), 0.04 μg/mL, and 4 μg/mL to determine the lowest-observed-adverse-effect level, or the LOAEL, which is the lowest concentration that causes an adverse alteration in cell viability. A dose-response assessment, a critical concept in toxicology and risk assessment, correlates a range of exposure doses or concentrations to a spectrum of induced effects, such as reduced cellular viability. Lower doses used within the dose-response assessment (i.e., 0.0004 μg/mL, 0.04 μg/mL) did not elicit a cell response nor any alterations in cell viability (i.e., reductions in cell viability) following a 48-hour exposure. From the dose-response assessment, it was determined that 4 μg/mL was the LOAEL and was used for each PM sample.

After the low and high doses were calculated using the MPPD program, PM stock solutions were diluted in PneumaCult™-Ex Plus media (STEMCELL™ Technologies, British Columbia, Canada). Dilution calculations depended on the initial concentrations, which varied for each sample based on the total PM mass collected in the field, and starting volumes, which were typically 500 to 600 μL (accounting for volume loss). Final volumes for the low and high doses for the reference control were calculated using 500 μg/mL as the starting concentration. Dilutions were performed aseptically (following GSU safety measures and protocols) by placing the correct volume of Ex Plus media into a plastic 15 mL conical tube, followed by the correct volume of particle stock solution into the media inside the tube. Diluted PM stock solutions were stored in a 4°C refrigerator until use.

3.4 SAE Cell Culture and Exposure

Small airway epithelial cells (SAEC; Lonza, Maryland, U.S.), which are targets in the inhalation route of traffic-related UFP exposure, were cultured in T-75 flasks using Ex Plus media ideal for SAEC to ensure colloidal stability and minimize agglomeration. SAEC were incubated in a controlled atmosphere of 37°C and 5% CO_2 until PM exposure. For PM exposures, SAEC were sub-cultured in 96-well plates at a density of 20,000 cells/mL and grown to 70-80% confluency. Confluency refers to the percentage of the surface area of each well covered with adherent cells. Previously prepared PM colloidal suspensions diluted in Ex Plus media were administered to SAEC for a period of 48 hours. The PM concentrations were matched to MPPD-calculated inhaled doses, which were administered to the SAEC.

After performing sample dilutions to replicate the calculated concentrations and preparing SAEC cultures, cultured cells were plated onto 96-well black plates (Corning Inc., New York, U.S.). Each well received 100 μL of particles containing exposure media, and each plate remained in the incubator for a 48-hour exposure period until toxicological assays were performed. Negative controls were prepared by using only Ex Plus media. Positive controls were prepared by diluting 1 μL of hydrogen peroxide (H_2O_2) into 999 μL of PBS (phosphate-buffered saline; STEMCELL™ Technologies, British Columbia, Canada). A second dilution was completed by adding 38.7 μL of the first dilution into 1 mL of PBS, which was then added to the cells fifteen minutes before beginning the assays. Blanks represented vehicle controls (i.e., MeOH solvent) and were prepared using (v/v) doses similar to PM exposures for the solvent vehicle to control for any excess MeOH present.

A plastic 15 mL conical tube was weighed in a small glass beaker and tared to prepare the reference control. The tube was then taken to a disinfected fume hood following GSU safety measures and protocols. Approximately 1 milligram (mg) of diesel particulate matter (industrial forklift, standard reference material 2975; National Institute of Standards and Technology [NIST], Maryland, U.S.) was placed inside the plastic tube using a spatula and weighed again. Approximately 1 mL of cell culture grade water (Corning Inc., New York, U.S.) was pipetted aseptically into the plastic tube, ensuring that any debris was washed off the sides of the tube (final concentration: 1 mg/mL). The tube, which contained a heterogenous mixture, was then sonicated in a cup sonicator at 75% amplitude for three minutes. The sonicator was filled with ice and water, securing the tube into place using tape. The reference control was stored in a 4°C refrigerator until use.

3.5 Toxicological Assays

3.5.1 Detecting Reactive Oxygen Species (ROS) Induction Using the CellROX® Assay

TRAP exposures produce ROS that exhibit lethal effects on viable, metabolically active cells (i.e., SAEC). ROS generation and subsequent interactions were detected and visualized using the CellROX® Oxidative Stress Orange Reagent (Invitrogen, California, U.S.), which localized in the cells' cytoplasm. After the cells were exposed to the various TRAP exposures, the reagent was prepared by aseptically adding 10 μL of the CellROX® Orange Reagent to 5 mL of PBS to create a 5 μM concentration, wrapping the plastic conical tube in aluminum foil until needed later. The treatments were removed from the cells, which were then washed twice with 200 μL of PBS. 50 μL of the prepared reagent was added to each well, and the 96-well plate was covered in aluminum foil and incubated for thirty minutes at 37°C. Following incubation, the media was removed, and

the cells were washed three times with 200 μL of PBS. Finally, using the Cytation 1 Cell Imaging Multi-Mode Reader (BioTek™ Instruments, Vermont, U.S.), the relative fluorescence intensities were measured and imaged at an excitation/emission maxima of ~ 545/565 nanometers (nm).

3.5.2 Detecting Total Glutathione (GSH) Using the GSH Assay

GSH is an antioxidant typically found in eukaryotic cells, an endogenous cellular metabolism component, and a tripeptide consisting of glycine, cysteine, and glutamic acid used to indicate oxidative stress, as observed by declines in total cellular GSH. The GSH/GSSG-Glo™ Assay (Promega, Wisconsin, U.S.) is a luminescence-based assay that detects and quantifies total glutathione (GSH and glutathione disulfide [GSSG] and GSSG levels as well as GSH-to-GSSG ratios in cultured cells, which served as a quantitative validation for the CellROX® assay in this study. 70 μL of Luciferin-NT, 70 μL of glutathione S-transferase (GST), and 7 mL of GSH/GSSG-Glo™ reaction buffer were added in a plastic 15 mL conical tube to prepare the GSH assay reagent. After removing the PM exposures/supernatants from each well and transferring them to a new, clean, and labeled 96-well plate, the cells were washed once with 200 μL of PBS. 50 μL of the prepared GSH reagent was added to each well, and the 96-well plate was incubated for thirty minutes. Then, 50 μL of the Luciferin detection reagent was added to each well for fifteen minutes, and the luminescence was measured within two hours using the Cytation 1 Cell Imaging Multi-Mode Reader.

3.5.3 Assessing Cellular Viability Using the MTS Assay

Cellular viability was assessed using a tetrazolium compound [3-(4,5-dimethylthiazol-2-yl)-5-(3-carboxymethoxyphenyl)-2-(4-sulfophenyl)-2H-tetrazolium, inner salt; MTS] in the MTS

colorimetric assay (CellTiter 96® AQ_{ueous} One Solution, Promega, Wisconsin, U.S.). The MTS assay detects the reduction of the MTS tetrazolium compound by viable mammalian cells to generate a colored formazan dye that is soluble in cell culture media. This conversion is thought to occur via NAD(P)H-dependent dehydrogenase enzymes in metabolically active cells. 777 μL of the MTS reagent was added into 6,223 μL of Ex-Plus media inside of a plastic 15 mL conical tube to prepare 7 mL of the MTS reagent (calculated using an 8x8 plating scheme in which 64 wells required 100 μL of the MTS reagent to total to approximately 6,400 μL of MTS reagent). After removing the PM exposures/supernatants from each well and transferring them to a new, clean, and labeled 96-well plate, the cells were washed once with 200 μL of PBS. Once the MTS reagent was added, the plate was placed inside the incubator for one to two hours. Absorbance measurements were made using the Cytation 1 Cell Imaging Multi-Mode Reader at an excitation/emission maximum of 490 nm. This same plate was also used for the GSH assay, also known as sequenced multiplexing.

3.6 Evaluation of Pro-Inflammatory Cytokines

Supernatants from previous experiments were stored in a -80°C freezer and used for cytokine analyses using the Human Cytokine Array Proinflammatory Focused 15-plex (HDF15; Eve Technologies, Alberta, Canada). The HDF15 was used to test for GM-CSF, IFNγ, IL-1β, IL-1ra, IL-2, IL-3, IL-4, IL-5, IL-6, IL-8, IL-10, IL-12(p40), IL-12(p70), MCP-1, and TNF-α using selected samples. The HDF15 examines human cytokines and chemokines, a particular cytokine type, using a multiplex immunoassay analyzed with a BioPlex 200 (Eve Technologies, 2021). Cytokines are key inflammation modulators, participating in acute and chronic inflammation via a complex network of interactions. Unlike hormones, cytokines act on a broader range of target

cells and are not produced by specialized cells (Eve Technologies, 2021). Cytokines and chemokines play an influential role in particle-mediated lung inflammation, such as that seen in allergic reactions and fibrosis (Moldoveanu et al., 2009; Robinson et al., 1993). Selected samples for cytokine analyses (Table 2) were prepared by centrifugation and were then aliquoted into 0.6 mL microcentrifuge tubes, labeled appropriately (T1 and T2 represent trials one and two, respectively), and shipped on dry ice.

3.7 Statistical Analyses

All exposures were evaluated in duplicates, and at least three experiments were conducted per toxicological assay. All data were normalized to the negative control and analyzed for significance using a one-way ANOVA analysis followed by Tukey's post-hoc test ($\alpha = 0.1$) utilizing GraphPad Prism software (Prism version 9.0.0). The one-way ANOVA analysis involving Tukey's post-hoc test included all ten treatment groups and the three control groups (i.e., negative control, positive control, low-dose reference control). P-values of less than or equal to 0.01 were deemed significant.

3.8 Materials and Reagents

The MeOH used to prepare 75% MeOH for PTFE filter extractions was purchased from Sigma Aldrich (Missouri, U.S.). PneumaCult™-Ex Plus media used to dilute PM stock solutions and culture SAEC was purchased from STEMCELL™ Technologies (British Columbia, Canada). SAEC were purchased from Lonza (Maryland, U.S.). 96-well black plates were purchased from Corning Inc. (New York, U.S.). The PBS used to prepare the negative control and blanks during toxicological experimentation was purchased from STEMCELL™ Technologies. The diesel

particulate matter (industrial forklift, standard reference material 2975) used to prepare the reference control was purchased from NIST (Maryland, U.S.). The cell culture grade water used to dilute the reference control to a concentration of 1 mg/mL was purchased from Corning Inc. (New York, U.S.).

The CellROX® Oxidative Stress Orange Reagent utilized during the CellROX® assay was purchased from Invitrogen (California, U.S.). The MTS reagent was prepared using CellTiter 96® AQ_{ueous} One Solution purchased from Promega (Wisconsin, U.S.). The GSH/GSSG-Glo™ Assay reagent was prepared utilizing Luciferin-NT, GST, and the GSH/GSSG-Glo™ reaction buffer purchased from Promega (Wisconsin, U.S.).

4. RESULTS

4.1 PTFE Filter Collection and Extraction Data

After the PTFE filters were reweighed following sample collection, the total particle mass collected on each filter was calculated by subtracting the average post-collection weight from the average pre-collection weight (in mg; Table 1). For example, sample TR2009 weighed 78.842 mg before sample collection and weighed 78.8735 mg after sample collection, yielding 0.0315 mg of total particle mass collected (Table 1). In addition to the particle mass collected for each sample filter, Table 1 also shows at which site and on what date the filters were collected. Each filter's position at the sites (i.e., road or barrier) is also listed. Except for S1, every site featured a barrier filter with less particle mass collected than the road filter. The average extraction efficiency calculated using selected samples (Table 1) was approximately 80.754%, which excludes an outlier (i.e., TR2009 with an extraction efficiency of roughly 479.365% likely due to a measurement error). Even though TR2009 was excluded from the average extraction efficiency calculations, it was still a valid measurement and was included in subsequent toxicological analyses since the initial concentration was diluted to match the MPPD-derived dose (4 μg/mL) like the other samples. The average extraction efficiency calculated using barrier samples (i.e., TR2022, TR2034, TR2037) was 74.694% (median: 77.231%) compared to the average extraction efficiency calculated using road samples (i.e., TR2011, TR2018, TR2019, TR2028, TR2030, TR2032), which was 83.784% (median: 85.431%).

4.2 Reactive Oxygen Species (ROS) Generation

Images revealing cell populations and associated oxidative stress induced by ROS production following the 48-hour exposures for specific samples were gathered (Figure 4). Figure

4 displays representative images for the controls, blanks, and selected samples from S1, S3, and S5 using the low dose (4 μg/mL). The blue stain represents DAPI signaling, and the orange stain represents Texas Red® signaling, which indicates oxidative stress via ROS generation. ROS production results in downstream alteration of membrane lipids, proteins, and nucleic acids (e.g., DNA). Subsequent oxidative damage of these biomolecules relates to several pathological events, including but not limited to respiratory illness (e.g., asthma, emphysema) and carcinogenesis.

The negative control does not exhibit any Texas Red® signaling, yet the positive and reference controls do, indicating oxidative stress (Figure 4). The blank reveals limited oxidative stress. Ideally, the negative control should reveal no oxidative stress, whereas positive controls should exhibit the highest amount of oxidative stress present in the cell population, with reference controls, blanks, and samples falling in between the negative and positive controls. Compared to the negative control, road and barrier PM mass resulted in decreased cell populations due to damaged and dying cells (Figure 4). When comparing road PM mass to barrier PM mass, however, a common trend included diminished Texas Red® signaling (i.e., reduced oxidative stress) observed following the barrier PM mass exposures. Samples TR2009 and TR2037 collected at S1 revealed increased oxidative stress compared to the other road-barrier pairs collected at S3 and S5.

4.3 Comparative Toxicological Assessments of PTFE Filter Extracted Mass

4.3.1 Low-Dose TRAP Exposures Elicit Oxidative Stress

Quantitative data summarizing antioxidant capacity using the GSH assay were gathered using the low dose (4 μg/mL; Figure 5). GSH regulates intracellular ROS by protecting cells against the damaging effects of oxidative stress and facilitating ROS cell signaling. When a GSH

imbalance occurs, the cell's oxidative stress response changes to reflect the pathogenesis of several adverse health outcomes, including asthma and fibrosis. Negative controls, positive controls, and low-dose reference controls are represented by black, grey, and blue bars, respectively (Figure 5). The x-axis represents the various treatment groups, whereas the y-axis represents percent control (Figure 5). For total GSH, the green bars indicate barrier PM mass, whereas the orange bars indicate road PM mass. Low doses using road PM mass did cause oxidative stress, as observed by a reduction in GSH levels at S1 and S5 (i.e., TR2009, TR2032, respectively). Figure 5 shows that barriers at these locations, however, reduced oxidative stress due to an increase in GSH levels (i.e., TR2037, TR2034, respectively).

4.3.2 The Impact of Low-Dose TRAP Exposures on Cellular Viability

Empirical data summarizing cellular viability using the MTS assay were gathered (Figure 5). NADPH-dependent dehydrogenase enzymes housed in the mitochondria induce the reduction of the tetrazolium compound in the MTS reagent to a colored formazan dye. The mitochondria's ability to employ these enzymes decreases as cellular viability declines. Negative controls, positive controls, and low-dose reference controls are represented by black, grey, and blue bars, respectively (Figure 5). The x-axis represents the various treatment groups, whereas the y-axis represents percent control (Figure 5). For cellular viability, the green bars indicate barrier PM mass, whereas the orange bars indicate road PM mass. Due to the low dose used (4 μg/mL), no overt toxicity was observed at most of the sites selected. Overall, there was no reduction in cellular viability at sites with barriers (e.g., S1, S3, S5), which compared barrier PM mass to road PM mass (i.e., TR2009 versus TR2037; TR2022 versus TR2019; TR2034 versus TR2032, respectively). In other words, most of the cells were still metabolically active and alive following the 48-hour

exposure period. For the S2 front-road PM mass (i.e., TR2011), however, more cells were inviable, indicating that cells either became damaged or died and could not metabolize the substrate – a formazan product – during the MTS assay or died. It proves crucial to note here that S2 did not contain barriers, only a chain-link fence between the service road and interstate (Figure 1). Barrier PM mass collected at S1 (i.e., TR2037) exhibited higher toxicity than road PM mass collected at the same site (i.e., TR2009; Figure 5).

4.4 Low-Dose TRAP Exposures Elicit Pro-inflammatory Cytokine Secretion

Increases in pro-inflammatory cytokines associated with airway inflammation were observed (Figure 6). Additionally, green barriers reduced pro-inflammatory cytokine secretion at specific sites (e.g., S3 and S5 for GM-CSF and TNF-α; S1, S3, and S5 for IL-8; and S1 and S5 for MCP-1). Negative controls, positive controls, and low-dose reference controls are represented by black, grey, and blue bars, respectively. The x-axis represents the various treatment groups, whereas the y-axis represents concentration (Figure 5). Green bars indicate barrier PM mass, whereas orange bars indicate road PM mass. Studies have indicated that GM-CSF likely contributes to airway remodeling and plays a crucial role in the pathogenesis of asthma (Saha et al., 2009). Barrier PM mass collected at S3 and S5 (i.e., TR2022, TR2034, respectively) resulted in a significant decrease in GM-CSF concentrations compared to road PM mass collected at the same sites (i.e., TR2019, TR2032, respectively; Figure 6A). Notably, the combination barrier (trees and sound wall) at S3 provided adequate protection against TRAP, given this observed reduction in GM-CSF concentrations. Even though a reduction in GM-CSF concentrations between front- versus side-road PM mass collected at S2 and S4 (i.e., TR2011 versus 2018;

TR2028 versus TR2030, respectively) was observed, this site contained no barriers (little to no trees present).

IL-8 is a biomarker for uncontrolled asthma and is considered a significant chemotactic factor, which involves neutrophil recruitment and activation (Ordoñez et al., 2000). It is also active on primed eosinophils. Barrier PM mass collected at S1, S3, and S5 (i.e., TR2037, TR2022, TR2034, respectively) resulted in a significant decrease in IL-8 concentrations compared to road PM mass collected at the same sites (i.e., TR2009, TR2022, TR2034, respectively; Figure 6B). In other words, any barrier type, such as a green or combination barrier, led to diminished IL-8 concentrations. The front-road PM mass collected at S2 (i.e., TR2011) exhibited decreased IL-8 concentrations than the side-road PM mass collected at the same site (i.e., TR2018).

Studies have indicated that monocyte chemotactic proteins (MCPs) in bronchoalveolar fluid are associated with the rapid appearance of a monocyte-derived population of alveolar macrophages (Lee et al., 2015). Barrier PM mass collected at S1 and S5 (i.e., TR2037, TR2034, respectively) resulted in a significant decrease in MCP-1 concentrations compared to road PM mass collected at the same sites (i.e., TR2009, TR2032, respectively; Figure 6C). Mainly, tree barriers provided sufficient protection against TRAP, given this observed reduction in MCP-1 concentrations. The front-road PM mass collected at S2 (i.e., TR2011) revealed lower MCP-1 concentrations than the side-road PM mass collected at the same site (i.e., TR2018). Conversely, the front-road PM mass collected at S4 (i.e., TR2028) exhibited higher MCP-1 concentrations than the side-road PM mass collected at the same site (i.e., TR2030).

TNF-α, a potent inflammatory cytokine, has been implicated in various pulmonary diseases, including asthma and emphysema (Keatings et al., 1997; Lucey et al., 2002). Barrier PM mass collected at S3 and S5 (i.e., TR2022, TR2034, respectively) resulted in a significant decrease in TNF-α concentrations compared to road PM mass collected at the same sites (i.e., TR2019, TR2032, respectively; Figure 6D). Unlike GM-CSF, however, the green barrier at S5 provided adequate protection against TRAP, given this observed reduction in TNF-α concentration. Like the other cytokines, the front-road PM mass collected at S2 (i.e., TR2011) exhibited decreased TNF-α concentrations than the side-road PM mass collected at the same site (i.e., TR2018).

5. DISCUSSION AND CONCLUSION

Low-level chronic doses of TRAP exposures may contribute to or exacerbate adverse health outcomes, including but not limited to asthma and inflammation, over time (Cesaroni et al., 2008; Guarnieri & Balmes, 2015; Huff, Carlsten, & Hirota, 2019; Landreman et al., 2008; Neophytou et al., 2013; Xia, Kovochich, & Nel, 2006). This study examined the toxicological profiles of traffic-related PM mass using SAEC to assess ROS generation, oxidative stress, antioxidant capacity, cellular viability, and cytokine secretion. Limited knowledge exists regarding green infrastructure and its influence on TRAP-mediated toxicological effects, and this study is the first of its kind to demonstrate the potential human health benefits of green barriers along major highways/roadways.

Site characteristics at S1 through S5 varied primarily based on barrier presence, temperature, precipitation, roadway layout, and traffic volume. While barriers featured at S1 and S5 included trees next to the major roadways, S2 and S4 did not have barriers, rather chain-link fences between the sampling stations and roadways. A combination barrier at S3, which included trees and a sound wall, was present. High temperatures (approximately 80-95°F) were observed at all examined sites. While sampling at S4 (i.e., on two different days: August 28 and September 10), the rain did not allow for a full day to gather data and collect PM mass. Regarding roadway layout and resulting traffic volume, S1's location was unique since two major roadways converge into one major roadway, contributing to increased traffic levels in the area (Afrin & Yodo, 2020), unlike the other examined sites. In addition to PM sampling using PTFE filters, extraction efficiencies following gravimetric analysis of total PM mass, typically around 80% (Kumar et al.,

2021), may correlate with the overall size distribution, indicating that smaller-sized particles are usually extracted more efficiently than larger-sized particles (Chen, Ji, & Zhao, 2019).

PM collected at various sites, including but not limited to urban areas with continuous traffic and stop-and-go traffic sites, has been shown to induce ROS generation (Li et al., 2003; Mirowsky et al., 2015) and increase pro-inflammatory potential (Mirowsky et al., 2013; Steenhof et al., 2011), especially in human lung epithelial cells (Li et al., 2002; Mazuryk, Stochel, & Brindell, 2020; Shi et al., 2006). ROS production and associated oxidative stress detected in selected barrier samples collected at S1, S3, and S5 revealed a reduction in ROS-induced oxidative stress when compared to selected road samples collected at the same sites. Oxidative stress, which refers to the imbalance between cellular antioxidants and oxidants, correlates with a cell's antioxidant capacity. Antioxidant capacity refers to a cell's ability to combat the oxidative damage done to it following a decline in the cellular GSH-to-GSSG ratio, which regulates and maintains redox balance (Li, Xia, & Nel, 2008). Changes in the GSH-to-GSSG ratio due to ROS production (Xia, Kovochich, & Nel, 2006) could initiate these stress responses that may injure the cells (Li, Xia, & Nel, 2008; Xia, Kovochich, & Nel, 2006). The oxidative potential of PM, or its ability to oxidize target molecules and exacerbate the imbalance between antioxidants and oxidants in favor of the latter, typically increased at sites with continuous traffic (Janssen et al., 2014). S1 samples TR2009 and TR2037 exhibited increased oxidative stress overall compared to other road-barrier pairs, likely due to S1's location and subsequent traffic volume.

Since limited sample concentrations were observed overall, it proved challenging to compare samples collected on the same day at the same site, specifically for S1 samples TR2009

and TR2037 as well as S2 samples TR2011 and TR2018. TR2037 was collected in September (compared to TR2009, which was collected in July), and the observed difference in ROS generation and resulting oxidative stress could have occurred due to varying traffic levels and temperature differences between those two months. Similarly, TR2011 was collected in late July (compared to TR2018, which was collected in early August), and the observed difference in oxidative stress could have occurred due to differing traffic levels between sampling days at S2. Low toxicity observed at most of the selected sites likely corresponded with low traffic volume present at each site (except for S1).

Observed oxidative stress in the collected CellROX® images complements the GSH and MTS assay data summarizing antioxidant capacity and cellular viability, respectively. Declines in total GSH levels observed in the road zones suggest an increase in oxidative stress caused by the low dose (4 μg/mL). Conversely, increases in GSH levels correspond with a reduction in oxidative stress, as observed in the barrier zones. As cellular ROS concentrations increase, antioxidant capacity typically declines, resulting in oxidative stress and an overall decrease in cellular viability for specific exposure durations (Huff, Carlsten, & Hirota, 2019; Landreman et al., 2008; Leikauf, Kim, & Jang, 2020). When traffic-related UFPs deposit in the airways, ROS production and oxidant-mediated cellular damage can occur, which can lead to adverse health effects (Huff, Carlsten, & Hirota, 2019; Leikauf, Kim, & Jang, 2020). Although changes in GSH levels occurred, a reduction in cellular viability at S1, S3, and S5 was not observed, indicating that the cell populations were still alive and metabolically active. Unlike the road PM mass collected at these sites, cells did not die or become damaged as often when exposed to barrier PM mass collected at these same sites. Following exposures using front-road PM mass collected at S2, the cells could

not survive the TRAP exposures at the dose and exposure duration. A decrease in cellular viability relates to an increase in TRAP-induced mechanisms, such as ROS production and oxidative (Cho et al., 2018; Lu et al., 2015). Generally, PM mass collected in the barrier zones did not reduce cellular viability as much as PM mass collected in the road zones, revealing the potential green infrastructure displays towards reducing TRAP-mediated respiratory effects.

Cellular cytokines and chemokines, which serve as modulators in TRAP-induced lung inflammation, increase in concentration in response to particle exposures and either solely employ inflammatory cells (e.g., IL-8) or recruit additional cytokines and chemokines or macrophages (e.g., TNF-α; Driscoll et al., 1997). Cytokine analyses that measured GM-CSF, IL-8, MCP-1, and TNF-α concentrations revealed that barrier TRAP did not elicit higher levels of cytokines than road TRAP. In other words, the cells secreted fewer cytokines in response to toxic insults using barrier PM mass. Leikauf, Kim, and Jang reported that UFP exposures promote cytokine secretion, especially for GM-CSF, IL-8, and TNF-α (2020). Generally, any barrier type (i.e., green or combination barrier) protected against TRAP, given observed reductions in GM-CSF, IL-8, MCP-1, and TNF-α concentrations. Interestingly, the barrier PM mass collected at S1 revealed increased GM-CSF and TNF-α concentrations compared to the road PM mass. These observed decreases in cytokine secretion complement the qualitative data the CellROX® assay provided and quantitative data the GSH assay provided. Viable and metabolically active cells with undisturbed antioxidant capacity do not secrete pro-inflammatory cytokines, whereas injured cells do (Leikauf, Kim, & Jang, 2020; Wieczfinska et al., 2019). Observed GSH levels as well as observed GM-CSF, IL-8, MCP-1, and TNF-α concentrations indicated that green barriers reduced TRAP-mediated effects on antioxidant capacity and cytokine secretion, respectively, in SAEC. Similarly, observed GM-

CSF, IL-8, and TNF-α concentrations revealed a combination barrier reduced TRAP-induced effects on cytokine secretion in SAEC.

Although this study offers preliminary evidence regarding PM exposures and how they can impact human cells, there are study limitations. Limited sample mass collection prevented assessment of cellular toxicity for identical days (especially at S1 and S2), which may have intervened with the cellular effects observed following exposures to PM collected at the examined sites. Due to the COVID-19 pandemic, reduced regional traffic levels led to decreased TRAP concentrations in the Atlanta area. Further analyses of this data should include data on traffic volume for each site. Similarly, the occurrence of rainfall impeded the collection of specific samples for a full day (approximately six hours) during the sampling campaign. These analyses do not include a full analysis of meteorological conditions, such as wind direction and windspeed, known to affect pollutant concentrations close to roadways.

In conclusion, green infrastructure may play a role in mitigating TRAP-mediated respiratory health effects. Over time, green barriers may lessen the toxicological impact caused by low-level chronic doses and reduce the occurrence of respiratory outcomes (e.g., inflammation). As urbanization continues, strategies to reduce exposures to motor vehicle emissions, such as installing porous and solid barriers, remain a top priority. Exploring the toxicological effects of traffic-related UFPs can offer valuable information regarding the mechanisms involved in TRAP-associated health effects and can be used in conjunction with continuous PM data and speciation. Investigating the mechanisms behind ROS generation, oxidative stress, antioxidant capacity, cellular viability, and cytokine secretion can also help understand TRAP-mediated health effects.

This study provides evidence to conduct future experiments regarding green infrastructure and its impact on traffic-related UFP exposures utilizing refined methodologies.

REFERENCES

Afrin, T., & Yodo, N. (2020). A survey of road traffic congestion measures towards a sustainable and resilient transportation system. *Sustainability*, *12*(11), 4660. https://doi.org/10.3390/su12114660

America Counts Staff. (2019). 2020 Census count guides funding of new roads and bridges. *U.S. Census Bureau*. Retrieved from https://www.census.gov/library/stories/2019/12/2020-census-count-guides-funding-of-new-roads-and-bridges.html

Amorim, J. H., Rodrigues, V., Tavares, R., Valente, J., & Borrego, C. (2013). CFD modelling of the aerodynamic effect of trees on urban air pollution dispersion. *Science of the Total Environment, 461-462*, 541-551. https://doi.org/10.1016/j.scitotenv.2013.05.031

Andersen, Z. J., Hvidberg, M., Jensen, S. S., Ketzel, M., Loft, S., Sørensen, M., Tjønneland, A., Overvad, K., & Raaschou-Nielsen, O. (2011). Chronic obstructive pulmonary disease and long-term exposure to traffic-related air pollution: A cohort study. *American Journal of Respiratory and Critical Care Medicine*, *183*(4), 455-461. https://doi.org/10.1164/rccm.201006-0937OC

Apelberg, B. J., Buckley, T. J., & White, R. H. (2005). Socioeconomic and racial disparities in cancer risk from air toxics in Maryland. *Environmental Health Perspectives*, *113*(6), 693-699. https://doi.org/10.1289/ehp.7609

Ash, M., & Fetter, T. R. (2004). Who lives on the wrong side of the environmental tracks? Evidence from the EPA's risk-screening environmental indicators model. *Social Science Quarterly*, *85*(2), 441-462. https://doi.org/10.1111/j.0038-4941.2004.08502011.x

Batterman, S., Ganguly, R., & Harbin, P. (2015). High resolution spatial and temporal mapping of traffic-related air pollutants. *International Journal of Environmental Research and Public Health, 12*(4), 3646-3666. https://doi.org/10.3390/ijerph120403646

Baldauf, R. (2016). *Recommendations for constructing roadside vegetation barriers to improve near-road air quality.* U.S. Environmental Protection Agency: Washington, D.C.

Beelen, R., Hoek, G., van den Brandt, P. A., Goldbohm, R. A., Fischer, P., Schouten, L. J., Armstrong, B., & Brunekreef, B. (2008). Long-term exposure to traffic-related air pollution and lung cancer risk. *Epidemiology, 19*(5), 702-710. https://doi.org/10.1097/EDE.0b013e318181b3ca

Boland, S., Bonvallot, V., Fournier, T., Baeza-Squiban, A., Aubier, M., & Marano, F. (2000). Mechanisms of GM-CSF increase by diesel exhaust particles in human airway epithelial cells. *American Journal of Physiology - Lung Cellular and Molecular Physiology, 278*(1), L25–L32. https://doi.org/10.1152/ajplung.2000.278.1.L25

Bowatte, G., Lodge, C., Lowe, A. J., Erbas, B., Perret, J., Abramson, M. J., Matheson, M., & Dharmage, S. C. (2015). The influence of childhood traffic-related air pollution exposure on asthma, allergy and sensitization: A systematic review and a meta-analysis of birth cohort studies. *Allergy, 70*(3), 245-256. https://doi.org/10.1111/all.12561

Brauer, M., Lencar, C., Tamburic, L., Koehoorn, M., Demers, P., & Karr, C. (2008). A cohort study of traffic-related air pollution impacts on birth outcomes. *Environmental Health Perspectives*, *116*(5), 680-686. https://doi.org/10.1289/ehp.10952

Bräuner, E. V., Forchhammer, L., Møller, P., Simonsen, J., Glasius, M., Wåhlin, P., Raaschou-Nielsen, O., & Loft, S. (2007). Exposure to ultrafine particles from ambient air and

oxidative stress-induced DNA damage. *Environmental Health Perspectives*, *115*(8), 1177-1182. https://doi.org/10.1289/ehp.9984

Brook, R. D., Franklin, B, Cascio, W., Hong, Y., Howard, G., Lipsett, M., Luepker, R., Mittleman, M., Samet, J., Smith, S. C. Jr., & Tager, I. (2004). Air pollution and cardiovascular disease: A statement for healthcare professionals from the Expert Panel on Population and Prevention Science of the American Heart Association. *Circulation*, *109*(21), 2655-2671. https://doi.org/10.1161/01.CIR.0000128587.30041.C8

Brook, R. D., Rajagopalan, S., Pope, C. A. III., Brook, J. R., Bhatnagar, A., Diez-Roux, A. V., Holguin, F., Hong, Y., Luepker, R. V., Mittleman, M. A., Peters, A., Siscovick, D., Smith, S. C. Jr., Whitesel, L., Kaufman, J. D., & American Heart Association Council on Epidemiology and Prevention, Council on the Kidney in Cardiovascular Disease, and Council on Nutrition, Physical Activity and Metabolism. (2010). Particulate matter air pollution and cardiovascular disease: An update to the scientific statement from the American Heart Association. *Circulation*, *121*(12), 2331-2378. https://doi.org/10.1161/CIR.0b013e3181dbece1

Brook, R. D., Urch, B., Dvonch, J. T., Bard, R. L., Speck, M., Keeler, G., Morishita, M., Marsik, F. J., Kamal, A. S., Kaciroti, N., Harkema, J., Corey, P., Silverman, F., Gold, D. R., Wellenius, G., Mittleman, M. A., Rajagopalan, S., & Brook, J. R. (2009). Insights into the mechanisms and mediators of the effects of air pollution exposure on blood pressure and vascular function in healthy humans. *Hypertension*, *54*(3), 659–667. https://doi.org/10.1161/HYPERTENSIONAHA.109.130237

Brugge, D., Patton, A. P., Bob, A., Reisner, E., Lowe, L., Bright, O. M., Durant, J. L., Newman, J., & Zamore, W. (2015). Developing community-level policy and practice to reduce

traffic-related air pollution exposure. *Environmental Justice*, *8*(3), 95-104. https://doi.org/10.1089/env.2015.0007

Carlsten, C., Salvi, S., Wong, G. W. K., & Chung, K. F. (2020). Personal strategies to minimize effects of air pollution on respiratory health: Advice for providers, patients, and the public. *European Respiratory Journal*, *55*(6), 1902056. https://doi.org/10.1183/13993003.02056-2019

Cesaroni, G., Badaloni, C., Porta, D., Forastiere, F., & Perucci, C. A. (2008). Comparison between various indices of exposure to traffic-related air pollution and their impact on respiratory health in adults. *Occupational & Environmental Medicine*, *65*(10), 683-690. https://doi.org/10.1136/oem.2007.037846

Cesaroni, G., Forastiere, F., Stafoggia, M., Andersen, Z. J., Badaloni, C., Beelen, R., Caracciolo, B., de Faire, U., Erbel, R., Eriksen, K. T., Fratiglioni, L., Galassi, C., Hampel, R., Heier, M., Hennig, F., Hilding, A., Hoffmann, B., Houthuijs, D., Jöckel, K. H., Korek, M., … Peters, A. (2014). Long term exposure to ambient air pollution and incidence of acute coronary events: Prospective cohort study and meta-analysis in 11 European cohorts from the ESCAPE Project. *BMJ (Clinical research ed.)*, *348*, f7412. https://doi.org/10.1136/bmj.f7412

Chen, C., Ji, W., & Zhao, B. (2019). Size-dependent efficiencies of ultrafine particle removal of various filter media. *Building and Environment*, *160*, 106171. https://doi.org/10.1016/j.buildenv.2019.106171

Chen, G., Wan, X., Yang, H., & Zou, X. (2015). Traffic-related air pollution and lung cancer: A meta-analysis. *Thoracic Cancer*, *6*(3), 307-318. https://doi.org/10.1111/1759-7714.12185

Chen, S., Tsai, C., Huang, C., Chen, H., Chen, S., Lin, C., Tsai, J., Chou, C. C., Lung, S. C., Huang, W., Roam, G., Wu, W., Smolik, J., & Dzumbova, L. (2010). Chemical mass closure and chemical characteristics of ambient ultrafine particles and other PM fractions. *Aerosol Science and Technology*, *44*(9), 713-723. https://doi.org/10.1080/02786826.2010.486385

Cheng, B., Wang-Li, L., Meskhidze, N., Classen, J., & Bloomfield, P. (2019). Spatial and temporal variations of $PM_{2.5}$ mass closure and inorganic $PM_{2.5}$ in the southeastern U.S. *Environmental Science and Pollution Research*, *26*(32), 33181-33191. https://doi.org/10.1007/s11356-019-06437-8

Chi, G. C., Hajat, A., Bird, C. E., Cullen, M. R., Griffin, B. A., Miller, K. A., Shih, R. A., Stefanick, M. L., Vedal, S., Whitsel, E. A., & Kaufman, J. D. (2016). Individual and neighborhood socioeconomic status and the association between air pollution and cardiovascular disease. *Environmental Health Perspectives*, *124*(12), 1840-1847. https://doi.org/10.1289/EHP199

Cho, H., Park, C., Shin, H., Park, K., & Lim, H. (2018). Comparison of the in vitro toxicological activity of various particulate matter. *Toxicological and Industrial Health*, *34*(2), 99-109. https://doi.org/10.1177/0748233717749694

Churg, A., Brauer, M., del Carmen Avila-Casado, M., Fortoul, T. I., & Wright, J. L. (2003). Chronic exposure to high levels of particulate air pollution and small airway remodeling. *Environmental Health Perspectives*, *111*(5), 714-718. https://doi.org/10.1289/ehp.6042

Cichon, M. A., & Radisky, D. C. (2014). ROS-induced epithelial-mesenchymal transition in mammary epithelial cells is mediated by NF-kB-dependent activation of Snail. *Oncotarget*, *5*(9), 2827-2838. https://doi.org/10.18632/oncotarget.1940

Clark, N. A., Demers, P. A., Karr, C. J., Koehoorn, M., Lencar, C., Tamburic, L., & Brauer, M. (2010). Effect of early life exposure to air pollution on development of childhood asthma. *Environmental Health Perspectives*, *118*(2), 284-290. https://doi.org/10.1289/ehp.0900916

Clifford, S., Mazaheri, M., Salimi, F., Ezz, W. N., Yeganeh, B., Low-Choy, S., Walker, K., Mengersen, K., Marks, G. B., & Morawska, L. (2018). Effects of exposure to ambient ultrafine particles on respiratory health and systemic inflammation in children. *Environment International*, *114*, 167-180. https://doi.org/10.1016/j.envint.2018.02.019

Cosselman, K. E., Allen, J., Jansen, K. L., Stapleton, P., Trenga, C. A., Larson, T. V., & Kaufman, J. D. (2020). Acute exposure to traffic-related air pollution alters antioxidant status in healthy adults. *Environmental Research*, *191*, 110027. https://doi.org/10.1016/j.envres.2020.110027

Crobeddu, B., Baudrimont, I., Deweirdt, J., Sciare, J., Badel, A., Camproux, A. C., Bui, L. C., & Baeza-Squiban, A. (2020). Lung antioxidant depletion: A predictive indicator of cellular stress induced by ambient fine particles. *Environmental Science & Technology*, *54*(4), 2360–2369. https://doi.org/10.1021/acs.est.9b05990

de Hartog, J. J., Hoek, G., Peters, A., Timonen, K. L., Ibald-Mulli, A., Brunekreef, B., Heinrich, J., Tittanen, P., van Wijnen, J. H., Kreyling, W., Kulmala, M., & Pekkanen, J. (2003). Effects of fine and ultrafine particles on cardiorespiratory symptoms in elderly subjects with coronary heart disease: The ULTRA study. *American Journal of Epidemiology*, *157*(7), 613-623. https://doi.org/10.1093/aje/kwg021

De Prins, S., Koppen, G., Jacobs, G., Dons, E., Van de Mieroop, E., Nelen, V., Fierens, F., Int Panis, L., De Boever, P., Cox, B., Nawrot, T. S., & Schoeters, G. (2013). Influence of

ambient air pollution on global DNA methylation in healthy adults: A seasonal follow-up. *Environment International, 59*, 418–424. https://doi.org/10.1016/j.envint.2013.07.007

Delphino, R. J., Tjoa, T., Gillen, D. L., Staimer, N., Polidori, A., Arhami, M., Jamner, L., Sioutas, C., & Longhurst, J. (2014). Traffic-related air pollution and blood pressure in elderly subjects with coronary artery disease. *Epidemiology, 21*(3), 393-404. https://doi.org/10.1097/EDE.0b013e3181d5e19b

Deng, Q., Lu, C., Yu, Y., Li, Y., Sundell, J., & Norbäck, D. (2016). Early life exposure to traffic-related air pollution and allergic rhinitis in preschool children. *Respiratory Medicine, 121*, 67-73. https://doi.org/10.1016/j.rmed.2016.10.016

Deshmane, S. L., Kremlev, S., Amini, S., & Sawaya, B. E. (2009). Monocyte chemoattractant protein-1 (MCP-1): An overview. *Journal of Interferon & Cytokine Research*, *29*(6), 313-326. https://doi.org/10.1089/jir.2008.0027

Driscoll, K. E., Carter, J. M., Hassenbein, D. G., & Howard, B. (1997). Cytokines and particle-induced inflammatory cell recruitment. *Environmental Health Perspectives*, *105*(Suppl. 5), 1159-1164. https://doi.org/10.1289/ehp.97105s51159

Dunhill, M. S. (1962). Postnatal growth of the lung. *Thorax*, *17*(4), 329-333. Retrieved from https://www.ncbi.nlm.nih.gov/pmc/articles/PMC1018719/

Eiseman, E. (1998). *Monitoring for Fine Particulate Matter*. RAND. Retrieved from http://www.rand.org/publications/MR/MR974

Eve Technologies. (2021). Human cytokine array proinflammatory focused 15-plex (HDF15). *Eve Technologies Corporation*. Retrieved from https://www.evetechnologies.com/product/human-cytokine-array-proinflammatory-focused-15-plex-hdf15/

Font, A., Baker, T., Mudway, I. S., Purdie, E., Dunster, C., Fuller, G. W. (2014). Degradation in urban air quality from construction activity and increased traffic arising from a road widening scheme. *Science of the Total Environment, 497-498*, 123-132. https://doi.org/10.1016/j.scitotenv.2014.07.060

Gallagher, J., Baldauf, R., Fuller, C. H., Kumar, P., Gill, L. W., & McNabola, A. (2015). Passive methods for improving air quality in the built environment: A review of porous and solid barriers. *Atmospheric Environment, 120*, 61-70. https://doi.org/10.1016/j.atmosenv.2015.08.075

Gasana, J., Dillikar, D., Mendy, A., Forno, E., & Vieira, E. R. (2012). Motor vehicle air pollution and asthma in children: A meta-analysis. *Environmental Research, 117*, 36-45. https://doi.org/10.1016/j.envres.2012.05.001

Gehring, U., Wijga, A. H., Brauer, M., Fischer, P., de Jongste, J. C., Kerkhof, M., Oldenwening, M., Smit, H. A., & Brunekreef, B. (2010). Traffic-related air pollution and the development of asthma and allergies during the first 8 years of life. *American Journal of Respiratory and Critical Care Medicine, 181*(6), 596-603. https://doi.org/10.1164/rccm.200906-0858OC

Gray, S. C., Edwards, S. E., & Miranda, M. L. (2013). Race, socioeconomic status, and air pollution exposure in North Carolina. Environmental Research, 126, 152-158. https://doi.org/10.1016/j.envres.2013.06.005

Guarnieri, M., & Balmes, J. R. (2015). Outdoor air pollution and asthma. *Lancet, 383*(9928), 1581-1592. https://doi.org/10.1016/S0140-6736(14)60617-6

Haghani, A., Johnson, R., Safi, N., Zhang, H., Thorwald, M., Mousavi, A., Woodward, N. C., Shirmohammadi, F., Coussa, V., Wise, J. P., Forman, H. J., Sioutas, C., Allayee, H.,

Morgan, T. E., & Finch, C. E. (2020). Toxicity of urban air pollution particulate matter in developing and adult mouse brain: Comparison of total and filter-eluted nanoparticles. *Environment International, 136,* 105510. https://doi.org/10.1016/j.envint.2020.105510

Health Effects Institute. (2010). *Traffic-related air pollution: A critical review of the literature on emissions, exposure, and health effects* (Report No. 17). Health Effects Institute. Retrieved from https://www.healtheffects.org/system/files/SR17TrafficReview.pdf

Hewitt, C. N., Ashworth, K., & MacKenzie, A. R. (2019). Using green infrastructure to improve urban air quality (GI4AQ). *Ambio, 49,* 62-73. https://doi.org/10.1007/s13280-019-01164-3

Hill, T. D., Jorgenson, A. K., Ore, P, Balistreri, K. S., & Clark, B. (2019). Air quality and life expectancy in the United States: An analysis of the moderating effect of income inequality. *SSM – Population Health, 7,* 100346. https://doi.org/10.1016/j.ssmph.2018.100346

Hooper, L. G., & Kaufman, J. D. (2018). Ambient air pollution and clinical implications for susceptible populations [Supplemental material]. *Annals of the American Thoracic Society, 15,* S64-S68. https://doi.org/10.1513/AnnalsATS.201707-574MG

Huff, R. D., Carlsten, C., & Hirota, J. A. (2019). An update on immunological mechanisms in the respiratory mucosa in response to air pollutants. *Journal of Allergy and Clinical Immunology, 143*(6), 1989-2001. https://doi.org/10.1016/j.jaci.2019.04.012

Ingram, D. D., & Franco, S. J. (2014). 2013 NCHS urban-rural classification scheme for counties. *Vital and Health Statistics 2, 166,* 1-73. Retrieved from https://www.cdc.gov/nchs/data/series/sr_02/sr02_166.pdf

Janssen, N. A. H., Yang, A., Strak, M., Steenhof, M., Hellack, B., Gerlofs-Nijland, M. E., Kuhlbusch, T., Kelly, F., Harrison, R., Brunekreef, B., Hoek, G., & Cassee, F. (2014). Oxidative potential of particulate matter collected at sites with different source characteristics. *Science of the Total Environment, 472*, 572-581. https://doi.org/10.1016/scitotenv.2013.11.099

Jantzen, K., Roursgaard, M., Desler, C, Loft, S., Rasmussen, L. J., & Møller, P. (2012). Oxidative damage to DNA by diesel exhaust particle exposure in co-cultures of human lung epithelial cells and macrophages. *Mutagenesis, 27*(6), 693-701. https://doi.org/10.1093/mutage/ges035

Jayasooriya, V. M., Ng, A. W. M., Muthukumaran, S., & Perera, B. J. C. (2017). Green infrastructure practices for improvement of urban air quality. *Urban Forestry & Urban Greening, 21*, 34-47: https://doi.org/10.1016/j.ufug.2016.11.007

Jerrett, M., Finkelstein, M. M., Brook, J. R., Arain, M. A., Kanaroglou, P., Stieb, D. M., Gilbert, N. L., Verma, D., Finkelstein, N., Chapman, K. R., & Sears, M. R. (2009). A cohort study of traffic-related air pollution and mortality in Toronto, Ontario, Canada. *Environmental Health Perspectives*, *117*(5), 772-777. https://doi.org/10.1289/ehp.11533

Ji, H., & Khurana Hershey, G. K. (2012). Genetic and epigenetic influence on the response to environmental particulate matter. *The Journal of Allergy and Clinical Immunology*, *129*(1), 33–41. https://doi.org/10.1016/j.jaci.2011.11.008

Jiang, H., Ahmed, C. M. S., Canchola, A., Chen, J. Y., & Lin, Y. (2019). Use of dithiothreitol assay to evaluate the oxidative potential of atmospheric aerosols. *Atmosphere, 10*(10), 571. https://doi.org/10.3390/atmos10100571

Jorgenson, A. K., Hill, T. D., Clark, B., Thombs, R. P., Ore, P., Balistreri, K. S., & Givens, J. E. (2020). Power, proximity, and physiology: Does income inequality and racial composition amplify the impacts of air pollution on life expectancy in the United States? *Environmental Research Letters*, *15*(2), 024013. https://doi.org/10.1088/1748-9326/ab6789

Kaufman, J. D., Adar, S. D., Barr, R. G., Budoff, M., Burke, G. L., Curl, C. L., Daviglus, M. L., Diez-Roux, A. V., Gassett, A. J., Jacobs, D. R., Kronmal, R., Larson, T. V., Navas-Acien, A., Olives, C., Sampson, P. D., Sheppard, L., Siscovick, D. S., Stein, J. H., Szpiro, A. A., & Watson, K. E. (2016). Association between air pollution and coronary artery calcification within six metropolitan areas in the USA (the Multi-Ethnic Study of Atherosclerosis and Air Pollution): A longitudinal cohort study. *Lancet, 388*(10045), 696-704. https://doi.org/10.1016/S0140-6736(16)00378-0

Kelly, F. J., & Fussell, J. C. (2012). Size, source, and chemical composition as determinants of toxicity attributable to ambient particulate matter. *Atmospheric Environment, 60*, 504-526. https://doi.org/10.1016/j.atmosenv.2012.06.039

Keatings, V. M., O'Connor, B. J., Wright, L. G., Huston, D. P., Corrigan, C. J., & Barnes, P. J. (1997). Late response to allergen is associated with increased concentrations of tumor necrosis factor-alpha and IL-5 in induced sputum. *Journal of Allergy and Clinical Immunology*, *99*(5), 693–698. https://doi.org/10.1016/s0091-6749(97)70032-0

Knoblauch, M. (2019). Americans spend 19 full work days a year stuck in traffic on their commute. *New York Times*. Retrieved from https://nypost.com/2019/04/19/americans-spend-19-full-work-days-a-year-stuck-in-traffic-on-their-commute/

Kumar, P., Kalaiarasan, G., Porter, A. E., Pinna, A., Kłosowski, M. M., Demokritou, P., Chung, K. F., Pain, C., Arvind, D. K., Arcucci, R., Adcock, I. M., & Dilliway, C. (2021). An overview of methods of fine and ultrafine particle collection for physicochemical characterisation and toxicity assessments. *Science of the Total Environment, 756*, 143553. https://doi.org/10.1016/j.scitotenv.2020.143553

Kuwayama, T., Ruehl, C. R., & Kleeman, M. J. (2013). Daily trends and source apportionment of ultrafine particulate mass ($PM_{0.1}$) over an annual cycle in a typical California city. *Environmental Science & Technology*, *47*(24), 13957-13966. https://doi.org/10.1021/es403235c

Kwon, H., Ryu, M. H., & Carlsten, C. (2020). Ultrafine particles: Unique physicochemical properties relevant to health and disease. *Experimental & Molecular Medicine*, *52*(3), 318-328. https://doi.org/10.1038/s12276-020-0405-1

Laeremans, M., Dons, E., Avila-Palencia, I., Carrasco-Turigas, G., Orjuela-Mendoza, J. P., Anaya-Boig, E., Cole-Hunter, T., de Nazelle, A., Nieuwenhuijsen, M. J., Standaert, A., van Poppel, M., de Boever, P., & Int Panis, L. (2018). Black carbon reduces the beneficial effect of physical activity on lung function. *Medicine and Science in Sports and Exercise*, *50*(9), 1875–1881. https://doi.org/10.1249/MSS.0000000000001632

Lakey, P. S. J., Berkemeier, T., Tong, H., Arangio, A. M., Lucas, K., Pöschl, U., & Shiraiwa, M. (2016). Chemical exposure-response relationship between air pollutants and reactive oxygen species in the human respiratory tract. *Scientific Reports*, *6*, 32916. https://doi.org/10.1038/srep32916

Landreman, A. P., Shafer, M. M., Hemming, J. C., Hannigan, M. P., & Schauer, J. J. (2008). A macrophage-based method for the assessment of the reactive oxygen species (ROS)

activity of atmospheric particulate matter (PM) and application to routine (daily-24 h) aerosol monitoring studies. *Aerosol Science and Technology*, *42*(11), 946-957. https://doi.org/10.1080/02786820802363819

Lanki, T., Pekkanen, J., Aalto, P., Elosua, R., Berglind, N., D'Ippoliti, D., Kulmala, M., Nyberg, F., Peters, A., Picciotto, S., Salomaa, V., Sunyer, J., Tiittanen, P., von Klot, S., & Forastiere, F. (2006). Associations of traffic related air pollutants with hospitalisation for first acute myocardial infarction: The HEAPSS study. *Occupational & Environmental Medicine*, *63*(12), 844–851. https://doi.org/10.1136/oem.2005.023911

Lee, Y. G., Jeong, J. J., Nyenhuis, S., Berdyshev, E., Chung, S., Ranjan, R., Karpurapu, M., Deng, J., Qian, F., Kelly, E. A., Jarjour, N. N., Ackerman, S. J., Natarajan, V., Christman, J. W., & Park, G. Y. (2015). Recruited alveolar macrophages, in response to airway epithelial-derived monocyte chemoattractant protein 1/CCl2, regulate airway inflammation and remodeling in allergic asthma. *American Journal of Respiratory Cell and Molecular Biology*, *52*(6), 772–784. https://doi.org/10.1165/rcmb.2014-0255OC

Leikauf, G. D., Kim, S., & Jang, A. (2020). Mechanisms of ultrafine particle-induced respiratory health effects. *Experimental & Molecular Medicine*, *52*(3), 329-337. https://doi.org/10.1038/s12276-020-0394-0

Li, Y., Duan, J., Yang, M., Li, Y., Jing, L., Yu, Y., Wang, J., & Sun, Z. (2017). Transcriptomic analyses of human bronchial epithelial cells BEAS-2B exposed to atmospheric fine particulate matter $PM_{2.5}$. *Toxicology in Vitro*, *42*, 171-181. https://doi.org/10.1016/j.tiv.2017.04.014

Li, N., Sioutas, C., Cho, A., Schmitz, D., Misra, C., Sempf, J. M., Wang, M., Oberley, T. D., Froines, J., & Nel, A. E. (2003). Ultrafine particle pollutants induce oxidative stress and

mitochondrial damage. *Environmental Health Perspectives*, *111*(4), 455-460. https://doi.org/10.1289/ehp.6000

Li, N., Wang, M., Oberley, T. D., Sempf, J. M., & Nel, A. E. (2002). Comparison of the pro-oxidative and proinflammatory effects of organic diesel exhaust particle chemicals in bronchial epithelial cells and macrophages. *The Journal of Immunology*, *169*(8), 4531-4541. https://doi.org/10.4049/jimmunol.169.8.4531

Li, N., Xia, T., & Nel, A. E. (2008). The role of oxidative stress in ambient particulate matter-induced lung diseases and its implications in the toxicity of engineered nanoparticles. *Free Radical Biology & Medicine*, *44*(9), 1689-1699. https://doi.org/10.1016/j.freeradbiomed.2008.01.028

Lindgren, A., Stroh, E., Montnémery, P., Nihlén, U., Jakobsson, K., & Axmon, A. (2009). Traffic-related air pollution associated with prevalence of asthma and COPD/chronic bronchitis. A cross-sectional study in Southern Sweden. *International Journal of Health Geographics*, *8*(1), 2. https://doi.org/10.1186/1476-072X-8-2

Ling, S. H., & van Eeden, S. F. (2009). Particulate matter air pollution exposure: Role in the development and exacerbation of chronic obstructive pulmonary disease. *International Journal of Chronic Obstructive Pulmonary Disease*, *4*, 233-243. https://doi.org/10.2147/copd.s5098

Link, M. S., & Dockery, D. W. (2010). Air pollution and the triggering of cardiac arrhythmias. *Current Opinion in Cardiology*, *25*(1), 16-22. https://doi.org/10.1097/HCO.0b013e32833358cd

Litschke, T., & Kuttler, W. (2008). On the reduction of urban particle concentration by vegetation – A review. *Meteorologische Zeitschrift, 17*(3), 229-240. https://doi.org/10.1127/0941-2948/2008/0284

Lu, S., Zhang, W., Zhang, R., Liu, P., Wang, Q., Shang, Y., Wu, M., Donaldson, K., & Wang, Q. (2015). Comparison of cellular toxicity caused by ambient ultrafine particles and engineered metal oxide nanoparticles. *Particle and Fibre Toxicology, 12*, 5. https://doi.org/10.1186/s12989-015-0082-8

Lucey, E. C., Keane, J., Kuang, P. P., Snider, G. L., & Goldstein, R. H. (2002). Severity of elastase-induced emphysema is decreased in tumor necrosis factor-alpha and interleukin-1beta receptor-deficient mice. *Laboratory Investigation, 82*(1), 79–85. https://doi.org/10.1038/labinvest.3780397

Lurmann, F., Avol, E., & Gilliland, F. (2015). Emissions reduction policies and recent trends in Southern California's ambient air quality. *Journal of the Air & Waste Management Association, 65*(3), 324-335. https://doi.org/10.1080/10962247.2014.991856

MacIntyre, E. A., Gehrin, U., Mölter, A., Fuertes, E., Klümper, C., Krämer, U., Quass, U., Hoffmann, B., Gascon, M., Brunekreef, B., Koppelman, G. H., Beelen, R. M. J., Hoek, G., Birk, M., de Jongste, J. C., Smit, H. A., Cyrys, J., Gruzieva, O., Korek, M., Bergström, A., Agius, R. M., de Vocht, F., Simpson, A., Porta, D., Forastiere, F., Badaloni, C., Cesaroni, G., Esplugues, A., Fernández-Somoano, A., Lerxundi, A., Sunyer, J., Cirach, M., Nieuwenhuijsen, M. J., Pershagen, G., & Heinrich, J. (2014). Air pollution and respiratory infections during early childhood: An analysis of 10 European birth cohorts within the ESCAPE project. *Environmental Health Perspectives, 122*(1), 107-113. https://doi.org/10.1289/ehp.1306755

Makri, A., & Stilianakis, N. I. (2008). Vulnerability to air pollution health effects. *International Journal of Hygiene and Environmental Health*, *211*(3-4), 326-336. https://doi.org/10.1016/j.ijheh.2007.06.005

Matz, C. J., Egyed, M., Hocking, R., Seenundun, S., Charman, N., & Edmonds, N. (2019). Human health effects of traffic-related air pollution (TRAP): A scoping review protocol. *Systematic Reviews*, *8*, 223. https://doi.org/10.1186/s13643-019-110605

Mazuryk, O., Stochel, G., & Brindell, M. (2020). Variations in reactive oxygen species generation by urban airborne particulate matter in lung epithelial cells-Impact of inorganic fraction. *Frontiers in Chemistry*, *8*, 581752. https://doi.org/10.3389/fchem.2020.581752

McConnell, R., Islam, T., Shankardass, K., Jerrett, M., Lurmann, F., Gilliland, F., Gauderman, J., Avol, E., Künzli, N., Yao, L., Peters, J., & Berhane, K. (2010). Childhood incident asthma and traffic-related air pollution at home and school. *Environmental Health Perspectives*, *118*(7), 1021-1026. https://doi.org/10.1289/ehp.0901232

Milando, C., Huang, L., & Batterman, S. (2016). Trends in $PM_{2.5}$ emissions, concentrations and apportionments in Detroit and Chicago. *Atmospheric Environment*, *129*, 197-209. https://doi.org/10.1016/j.atmosenv.2016.01.012

Mirowsky, J. E., Hickey, C., Horton, L., Blaustein, M., Galdanes, K., Peltier, R. E., Chillrud, S., Chen, L. C., Ross, J., Nadas, A., Lippmann, M., & Gordon, T. (2013). The effect of particle size, location and season on the toxicity of urban and rural particulate matter. *Inhalation Toxicology*, *25*(13), 747-757. https://doi.org/10.3109/08958378.2013.846443

Mirowsky, J. E., Jin, L., Thurston, G., Lighthall, D., Tyner, T., Horton, L., Galdanes, K., Chillrud, S., Ross, J., Pinkerton, K. E., Chen, L. C., Lippmann, M., & Gordon, T. (2015).

In vitro and in vivo toxicity of urban and rural particulate matter from California. *Atmospheric Environment, 103,* 256-262. https://doi.org/10.1016/j.atmosenv.2014.12.051

Moldoveanu, B., Otmishi, P., Jani, P., Walker, J., Sarmiento, X., Guardiola, J., Saad, M., & Yu, J. (2009). Inflammatory mechanisms in the lung. *Journal of Inflammation Research, 2,* 1-11. Retrieved from https://www.ncbi.nlm.nih.gov/pmc/articles/PMC3218724/#:~:text=Cytokines%20are%20produced%20by%20a,and%20immunoregulatory%20Th2%20cytokines%20dominate

Møller, P., & Loft, P. (2010). Oxidative damage to DNA and lipids as biomarkers of exposure to air pollution. *Environmental Health Perspectives, 118*(8), 1126-1136. https://doi.org/10.1289/ehp.0901725

Morishita, M., Keeler, G. J., Wagner, J. G., & Harkema, J. R. (2006). Source identification of ambient $PM_{2.5}$ during summer inhalation exposure studies in Detroit, MI. *Atmospheric Environment, 40*(21), 3823-3834. https://doi.org/10.1016/j.atmosenv.2006.03.005

Neophytou, A. M., Hart, J. E., Cavallari, J. M., Smith, T. J., Dockery, D. W., Coull, B. A., Garshick, E., & Laden, F. (2013). Traffic-related exposures and biomarkers of systemic inflammation, endothelial activation and oxidative stress: A panel study in the US trucking industry. *Environmental Health, 12,* 105. https://doi.org/10.1186/1476-069X-12-105

Nussbaumer, T., Czasch, C., Klippel, N., Johansson, L., & Tullin, C. (2008). Particulate emissions from biomass combustion in IEA countries: Survey on measurements and emission factors. *International Energy Agency*. Retrieved from http://citeseerx.ist.psu.edu/viewdoc/download?doi=10.1.1.614.4334&rep=rep1&type=pdf

Nuvolone, D., della Maggiore, R., Maio, S., Fresco, R., Baldacci, S., Carrozzi, L., Pistelli, F., & Viegi, G. (2011). Geographical information system and environmental epidemiology: A cross-sectional spatial analysis of the effects of traffic-related air pollution on population respiratory health. *Environmental Health*, *10*, 12. https://doi.org/10.1186/1476-069x-10-12

O'Neill, M. S., Jerrett, M., Kawachi, I., Levy, J. I., Cohen, A. J., Gouveia, N., Wilkinson, P., Fletcher, T., Cifuentes, L., Schwartz, J., & Workshop on Air Pollution and Socioeconomic Conditions. (2003). Health, wealth, and air pollution: Advancing theory and methods. *Environmental Health Perspectives*, *111*(16), 1861-1870. https://doi.org/10.1289/ehp.6334

Ordoñez, C. L., Shaughnessy, T. E., Matthay, M. A., & Fahy, J. V. (2000). Increased neutrophil numbers and IL-8 levels in airway secretions in acute severe asthma: Clinical and biologic significance. *American Journal of Respiratory and Critical Care Medicine*, *161*(4 Pt 1), 1185–1190. https://doi.org/10.1164/ajrccm.161.4.9812061

Ostro, B. D., Feng, W., Broadwin, R., Malig, B. J., Green, R. S., & Lipsett, M. J. (2008). The impact of components of fine particulate matter on cardiovascular mortality in susceptible subpopulations. *Occupational and Environmental Medicine*, *65*(11), 750-756. https://doi.org/10.1136/oem.2007.036673

Ostro, B. D., Roth, L., Malig, B. J., & Marty, M. (2009). The effects of fine particle components on respiratory hospital admissions in children. *Environmental Health Perspectives*, *117*(3), 475-480. https://doi.org/10.1289/ehp.11848

Park, Y. M., & Kwan, M. (2020). Understanding racial disparities in exposure to traffic-related air pollution: Considering the spatiotemporal dynamics of population distribution.

International Journal of Environmental Research and Public Health, *17*(3), 908. https://doi.org/10.3390/ijerph17030908

Power, M. C., Adar, S. D., Yanosky, J. D., & Weuve, J. (2016). Exposure to air pollution as a potential contributor to cognitive function, cognitive decline, brain imaging, and dementia: A systematic review of epidemiologic research. *Neurotoxicology*, *56*, 235-253. https://doi.org/10.1016/j.neuro.2016.06.004

Ray, P. D., Huang, B., & Tsuji, Y. (2012). Reactive oxygen species (ROS) homeostasis and redox regulation in cellular signaling. *Cellular Signalling*, *24*(5), 981-990. https://doi.org/10.1016/j.cellsig.2012.01.008

Raz, R., Roberts, A. L., Lyall, K., Hart, J. E., Just, A. C., Laden, F., & Weisskopf, M. G. (2015). Autism spectrum disorder and particulate matter air pollution before, during, and after pregnancy: A nested case-control analysis within the Nurses' Health Study II cohort. *Environmental Health Perspectives*, *123*(3), 264-270. https://doi.org/10.1289/ehp.1408133

Raza, W., Forsberg, B., Johansson, C., & Sommar, J. N. (2018). Air pollution as a risk factor in health impact assessments of a travel mode shift towards cycling. *Global Health Action*, *11*(1), 1429081. https://doi.org/10.1080/16549716.2018.1429081

Risom, L., Møller, P., & Loft, S. (2005). Oxidative stress-induced DNA damage by particulate air pollution. *Mutation Research*, *592*(1-2), 119-137. https://doi.org/10.1016/j.mrfmmm.2005.06.012

Robinson, D., Hamid, Q., Bentley, A., Ying, S., Kay, A. B., & Durham, S. R. (1993). Activation of CD4+ T cells, increased TH2-type cytokine mRNA expression, and eosinophil recruitment in bronchoalveolar lavage after allergen inhalation challenge in patients with

atopic asthma. *Journal of Allergy and Clinical Immunology*, *92*(2), 313-324. https://doi.org/10.1016/0091-6749(93)90175-f

Roper, C., Delgado, L. S., Barrett, D., Simonich, S. L. M., & Tanguay, R. L. (2020). $PM_{2.5}$ filter extraction methods: Implications for chemical and toxicological analyses. *Environmental Science & Technology*, *53*(1), 434-442. https://doi.org/10.1021/acs.est.8b04308

Rosanna, D. P., & Salvatore, C. (2012). Reactive oxygen species, inflammation, and lung diseases. *Current Pharmaceutical Design*, *18*(26), 3889-3900. https://doi.org/10.2174/138161212802083716

Saha, S., Doe, C., Mistry, V., Siddiqui, S., Parker, D., Sleeman, M., Cohen, E. S., & Brightling, C. E. (2009). Granulocyte-macrophage colony-stimulating factor expression in induced sputum and bronchial mucosa in asthma and COPD. *Thorax*, *64*(8), 671–676. https://doi.org/10.1136/thx.2008.108290

Samek, L. (2016). Overall human mortality and morbidity due to exposure to air pollution. *International Journal of Occupational Medicine and Environmental Health*, *29*(3), 417-426. https://doi.org/10.13075/ijomeh.1896.00560

Sawyer, K., Mundandhara, S., Ghio, A. J., & Madden, M. C. (2010). The effects of ambient particulate matter on human alveolar macrophage oxidative and inflammatory responses. *Journal of Toxicology and Environmental Health - Part A*, *73*(1), 41–57. https://doi.org/10.1080/15287390903248901

Shi, T., Duffin, R., Borm, P. J. A., Li, H., Weishaupt, C., & Schins, R. P. F. (2006). Hydroxyl-radical-dependent DNA damage by ambient particulate matter from contrasting sampling locations. *Environmental Research*, *101*(1), 18-24. https://doi.org/10.1016/j.envres.2005.09.005

Silbajoris, R., Osornio-Vargas, A. R., Simmons, S. O., Reed, W., Bromberg, P. A., Dailey, L. A., & Samet, J. M. (2011). Ambient particulate matter induces interleukin-8 expression through an alternative NF-κB (nuclear factor-kappa B) mechanism in human airway epithelial cells. *Environmental Health Perspectives, 119*(10), 1379–1383. https://doi.org/10.1289/ehp.1103594

Sohrabi, S., Zietsman, J., & Khreis, H. (2020). Burden of disease assessment of ambient air pollution and premature mortality in urban areas: The role of socioeconomic status and transportation. International Journal of Environmental Research and Public Health, *17*(4), 1166. https://doi.org/10.3390/ijerph17041166

Solomon, P. A., & Sioutas, C. (2008). Continuous and semicontinuous monitoring techniques for particulate matter mass and chemical components: A synthesis of findings from EPA's Particulate Matter Supersites Program and related studies. *Journal of the Air & Waste Management Association, 58*(2), 164-195. https://doi.org/10.3155/1047-3289.58.2.164

Stafoggia, M., Cesaroni, G., Peters, A., Andersen, Z. J., Badaloni, C., Beelen, R., Caracciolo, B., Cyrys, J., de Faire, U., de Hoogh, K., Eriksen, K. T., Fratiglioni, L., Galassi, C., Gigante, B., Havulinna, A. S., Hennig, F., Hilding, A., Hoek, G., Hoffmann, B., Houthuijs, D., … Forastiere, F. (2014). Long-term exposure to ambient air pollution and incidence of cerebrovascular events: Results from 11 European cohorts within the ESCAPE project. *Environmental Health Perspectives*, *122*(9), 919–925. https://doi.org/10.1289/ehp.1307301

Steenhof, M., Gosens, I., Strak, M., Godri, K. J., Hoek, G., Cassee, F. R., Mudway, I. S., Kelly, F. J., Harrison, R. M., Lebret, E., Brunekreef, B., Janssen, N. A. H., & Pieters, R. H. H. (2011). In vitro toxicity of particulate matter (PM) collected at different sites in the

Netherlands is associated with PM composition, size fraction and oxidative potential – the RAPTES project. *Particle and Fibre Toxicology*, *8*(26). https://doi.org/10.1186/1743-8977-8-26

Strosnider, H., Kennedy, C., Monti, M., & Yip, F. (2017). Rural and urban differences in air quality, 2008-2012, and community drinking water quality, 2010-2015 – United States. *Morbidity and Mortality Weekly Report (MMWR): Surveillance Summaries I*, *66*(13), 1-10. https://doi.org/10.15585/mmwr.ss6613a1

Sydbom, A., Blomberg, A., Parnia, S., Stenfors, N., Sandström, T., & Dahlén, S. E. (2001). Health effects of diesel exhaust emissions. *European Respiratory Journal*, *17*(4), 733-746. https://doi.org/10.1183/09031936.01.17407330

Tessum, C. W., Apte, J. S., Goodkind, A. L., Muller, N. Z., Mullins, K. A., Paolella, D. A., Polasky, S., Springer, N. P. Thakrar, S. K., Marshall, J. D., & Hill, J. D. (2019). Inequity in consumption of goods and services adds to racial-ethnic disparities in air pollution exposure. *Proceedings of the National Academy of Sciences of the United States of America*, *116*(13), 6001-6006. https://doi.org/10.1073/pnas.1818859116

Thomson, E. M., Breznan, D., Karthikeyan, S., MacKinnon-Roy, C., Charland, J., Dabek-Zlotorzynska, E., Celo, V., Kumarathasan, P., Brook, J. P., & Vincent, R. (2015). Cytotoxic and inflammatory potential of size-fractionated particulate matter collected repeatedly within a small urban area. *Particle and Fibre Toxicology*, *12*, 24. https://doi.org/10.1186/s12989-015-0099-z

Tian, N., Xue, J., & Barzyk, T. M. (2012). Evaluation socioeconomic and racial differences in traffic-related metrics in the United States using a GIS approach. *Journal of Exposure Science & Environmental Epidemiology*, *23*, 215-222. https://doi.org/10.1038/jes.2012.83

United Nations. (2014). World urbanization prospects: The 2018 revision. Geneva, Switzerland: 2014. Retrieved from https://population.un.org/wup/Publications/Files/WUP2018-KeyFacts.pdf

University of Washington Institute for Health Metrics and Evaluation. (2016). GBD compare data visualization. Retrieved from http://www.healthdata.org/data-visualization/gbd-compare

U.S. Bureau of Labor Statistics. (2020). Average hours per day spent in primary activities for the civilian population, 2019 quarterly and annual averages. *U.S. Department of Labor*. Retrieved from https://www.bls.gov/news.release/atus.t12.htm

U.S. Bureau of Transportation Statistics. (n.d.). Number of U.S. aircraft, vehicles, vessels, and other conveyances. *United States Department of Transportation*. Retrieved from https://www.bts.gov/content/number-us-aircraft-vehicles-vessels-and-other-conveyances

U.S. Census Bureau. (2019). 2019 U.S. population estimates continue to show the nation's growth is slowing. Retrieved from https://www.census.gov/newsroom/press-releases/2019/popest-nation.html#:~:text=The%20nation's%20population%20was%20328%2C239%2C523,multiyear%20slowdown%20since%20that%20period

U.S. Environmental Protection Agency. (2011). Inhalation rates. *Exposure factors handbook*. U.S. Environmental Protection Agency. Retrieved from https://www.epa.gov/sites/production/files/2015-09/documents/efh-chapter06.pdf

U.S. Environmental Protection Agency. (2016). NAAQS table. Retrieved from https://www.epa.gov/criteria-air-pollutants/naaqs-

table#:~:text=Primary%20standards%20provide%20public%20health,crops%2C%20vegetation%2C%20and%20buildings

U.S. Environmental Protection Agency. (2019). Our nation's air: Status and trends through 2018. Retrieved from https://gispub.epa.gov/air/trendsreport/2019/

U.S. Environmental Protection Agency. (2020). Air quality – National summary. Retrieved from https://www.epa.gov/air-trends/air-quality-national-summary

U.S. Environmental Protection Agency. (2020). Our nation's air: Status and trends through 2019. Retrieved from https://gispub.epa.gov/air/trendsreport/2020/

U.S. Environmental Protection Agency. (2020). Research on near roadway and other near source air pollution. Retrieved from https://www.epa.gov/air-research/research-near-roadway-and-other-near-source-air-pollution

Venekatachari, P., & Hopke, P. K. (2008). Development and laboratory testing of an automated monitor for the measurement of atmospheric particle-bound reactive oxygen species (ROS). *Aerosol Science and Technology, 42*(8), 629-635. https://doi.org/10.1080/02786820802227345

Verma, V., Fang, T., Xu, L., Peltier, R. E., Russell, A. G., Ng, N. L., & Weber, R. J. (2015). Organic aerosols associated with the generation of reactive oxygen species (ROS) by water-soluble $PM_{2.5}$. *Environmental Science & Technology, 49*(7), 4646-4656. https://doi.org/10.1021/es505577w

Vimercati, L. (2011). Traffic related air pollution and respiratory morbidity. *Lung India*, *28*(4), 238. https://doi.org/10.4103/0970-2113.85682

Wang, M., Aaron, C. P., Madrigano, J., Hoffman, E. A., Angelini, E., Yang, J., Laine, A., Vetterli, T. M., Kinney, P. L., Sampson, P. D., Sheppard, L. E., Szpiro, A. A., Adar, S.

D., Kirwa, K., Smith, B., Lederer, D. J., Diez-Roux, A. V., Vedal, S., Kaufman, J. D., & Barr, R. G. (2019). Association between long-term exposure to ambient air pollution and change in quantitatively assessed emphysema and lung function. *JAMA*, *322*(6), 546–556. https://doi.org/10.1001/jama.2019.10255

Wang, R., Henderson, S. B., Sbihi, H., Allen, R. W., & Brauer, M. (2013). Temporal stability of land use regression models for traffic-related air pollution. *Atmospheric Environment*, *64*, 312-319. https://doi.org/10.1016/j.atmosenv.2012.09.056

Wieczfinska, J., Sitarek, P., Skała, E., Kowalczyk, T., & Pawliczak, R. (2019). Inhibition of NADPH oxidase-derived reactive oxygen species decreases expression of inflammatory cytokines in A549 cells. *Inflammation*, *42*(6), 2205-2214. https://doi.org/10.1007/s10753-019-01084-0

Wilson, W. E., Chow, J. C., Claiborn, C., Fusheng, W., Engelbrecht, J., & Watson, J. G. (2002). Monitoring of particulate matter outdoors. *Chemosphere*, *49*(9), 1009-1043. https://doi.org/10.1016/S0045-6535(02)00270-9

Wu, J., Shi, Y., Asweto, C. O., Feng, L., Yang, X., Zhang, Y., Hu, H., Duan, J., & Sun, Z. (2017). Fine particle matters induce DNA damage and G2/M cell cycle arrest in human bronchial epithelial BEAS-2B cells. *Environmental Science and Pollution Research International*, *24*(32), 25071–25081. https://doi.org/10.1007/s11356-017-0090-3

Xia, T., Kovochich, M., & Nel, A. E. (2006). The role of reactive oxygen species and oxidative stress in mediating particulate matter injury. *Clinics in Occupational and Environmental Medicine*, *5*(4), 817–836. https://doi.org/10.1016/j.coem.2006.07.005

Xia, T., Nitschke, M., Zhang, Y., Shah, P., Crabb, S., & Hansen, A. (2015). Traffic-relation air pollution and health co-benefits of alternative transport in Adelaide, South Australia. *Environment International*, *74*, 281-290. https://doi.org/10.1016/j.envint.2014.10.004

Yorifuji, T., Kashima, S., Higa Diez, M., Kado, Y., Sanada, S., & Doi, H. (2016). Prenatal exposure to traffic-related air pollution and child behavioral development milestone delays in Japan. *Epidemiology*, *27*(1), 57-65. https://doi.org/10.1097/EDE.0000000000000361

Zhang, J. M., & An, J. (2007). Cytokines, inflammation, and pain. *International Anesthesiology Clinics*, *45*(2), 27–37. https://doi.org/10.1097/AIA.0b013e318034194e

TABLES

Table 1. Collected and Extracted Particle Mass Using Selected Sample Filters

Site ID	Date Collected	PTFE Filter ID	Road versus Barrier	Particle Mass Collected (mg)	Particle Mass Extracted (mg)	Extraction Efficiency (%)
S1	7/24/20	TR2009	Road	0.0315	0.151	479.3650794
S1	9/3/20	TR2037	Barrier	0.1625	0.1255	77.23076923
S2	7/28/20	TR2011	NA (Front-Road)	0.4895	0.425	86.82328907
S2	8/7/20	TR2018	NA (Side-Road)	0.1655	0.149	90.03021148
S3	8/20/20	TR2019	Road	0.1175	0.1	85.10638298
S3	8/20/20	TR2022	Barrier	0.054	0.0325	60.18518519
S4	8/28/20	TR2028	NA (Front-Road)	0.0505	0.043	85.14851485
S4	8/28/20	TR2030	NA (Side-Road)	0.028	0.024	85.71428571
S5	9/1/20	TR2032	Road	0.0415	0.029	69.87951807
S5	9/1/20	TR2034	Barrier	0.015	0.013	86.66666667

Table 2. Selected Samples Sent to Eve Technologies for Cytokine Analyses (HDF15)

Site ID	Date Collected	ET Sample ID (T1)	ET Sample ID (T2)	Road versus Barrier
S1	7/17/20	2004L T1	2004L T2	Barrier
S1	7/22/20	2005L T1	2005L T2	Barrier
S1	7/24/20	2008L T1	2008L T2	Barrier
S1	7/24/20	2009L T1	2009L T2	Road
S1	9/3/20	2035L T1	2035L T2	Road
S1	9/3/20	2037L T1	2037L T2	Barrier
S2	7/28/20	2011L T1	2011L T2	NA (Front-Road)
S2	7/28/20	2014L T1	2014L T2	NA (Side-Road)
S2	8/7/20	2018L T1	2018L T2	NA (Side-Road)
S3	8/20/20	2019L T1	2019L T2	Road
S3	8/20/20	2022L T1	2022L T2	Barrier
S4	8/28/20	2028L T1	2028L T2	NA (Front-Road)
S4	8/28/20	2030L T1	2030L T2	NA (Side-Road)
S5	8/27/20	2023L T1	2023L T2	Road
S5	8/27/20	2025L T1	2025L T2	Barrier
S5	9/1/20	2032L T1	2032L T2	Road
S5	9/1/20	2034L T1	2034L T2	Barrier
S1	7/22/20	FB2001 T1	FB2001 T2	
		NC T1	NC T2	
		PC T1	PC T2	
		RL T1	RL T2	
		BL T1	BL T2	

FIGURES

Figure 1. Mobile Cart Featuring Continuous Instrumentation at S2

Figure 2. Cascade Particle Impactor and Weather Station Set-up at S1

Figure 3. Map of All Site Locations (S1-S5) in Atlanta, GA

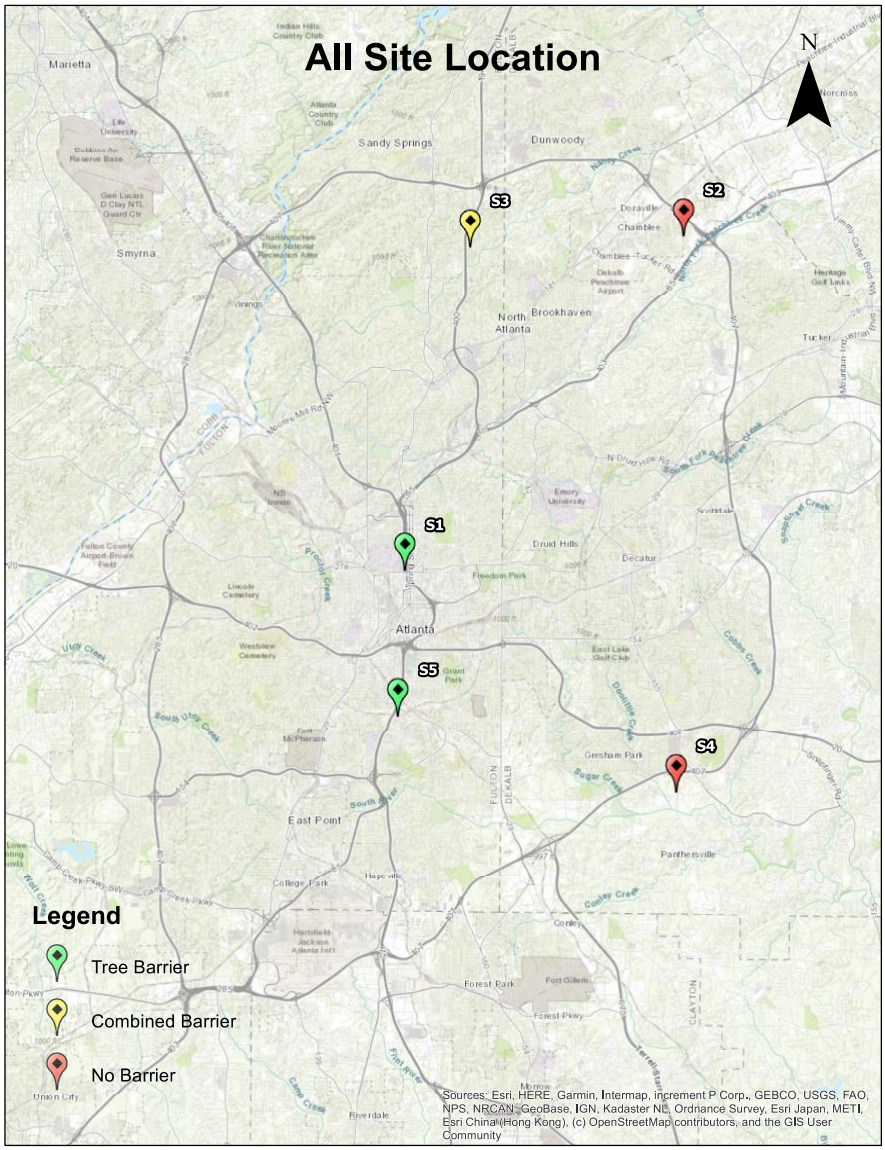

Figure 4. Reactive Oxygen Species Generation After 48-Hour Exposure Using CellROX® Images for S1, S3, and S5

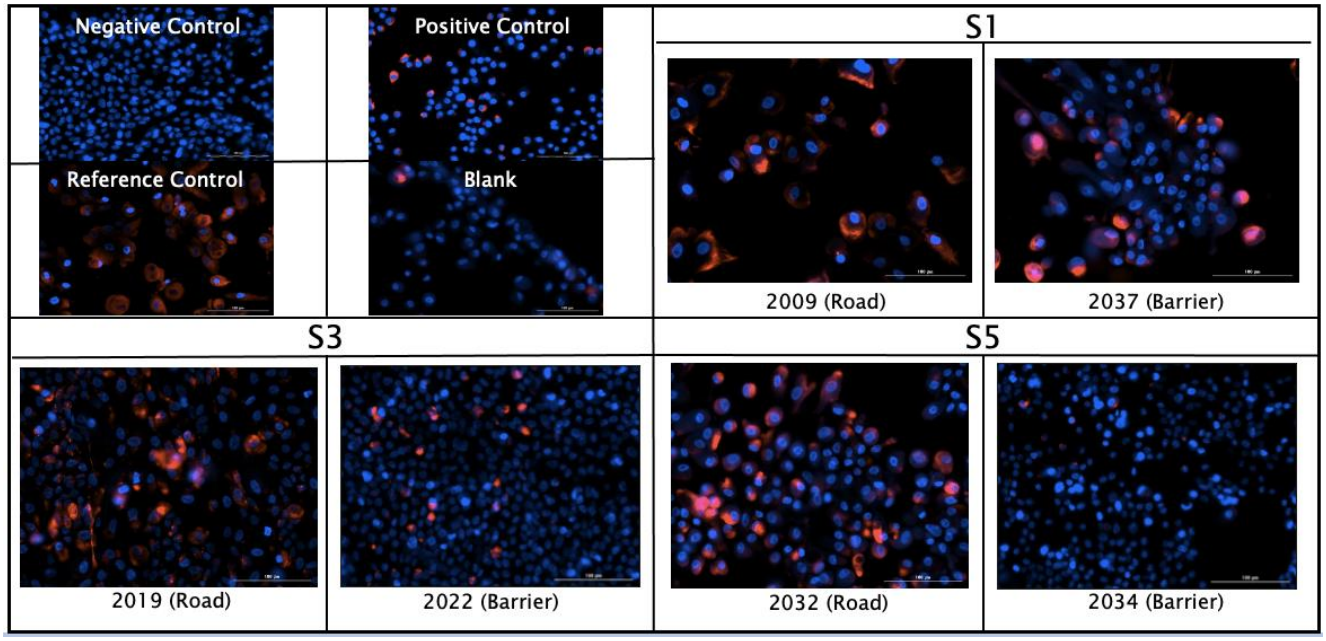

Figure 5. The Impact of TRAP on Oxidative Stress in Small Airway Epithelial Cells and Corresponding Cell Viability

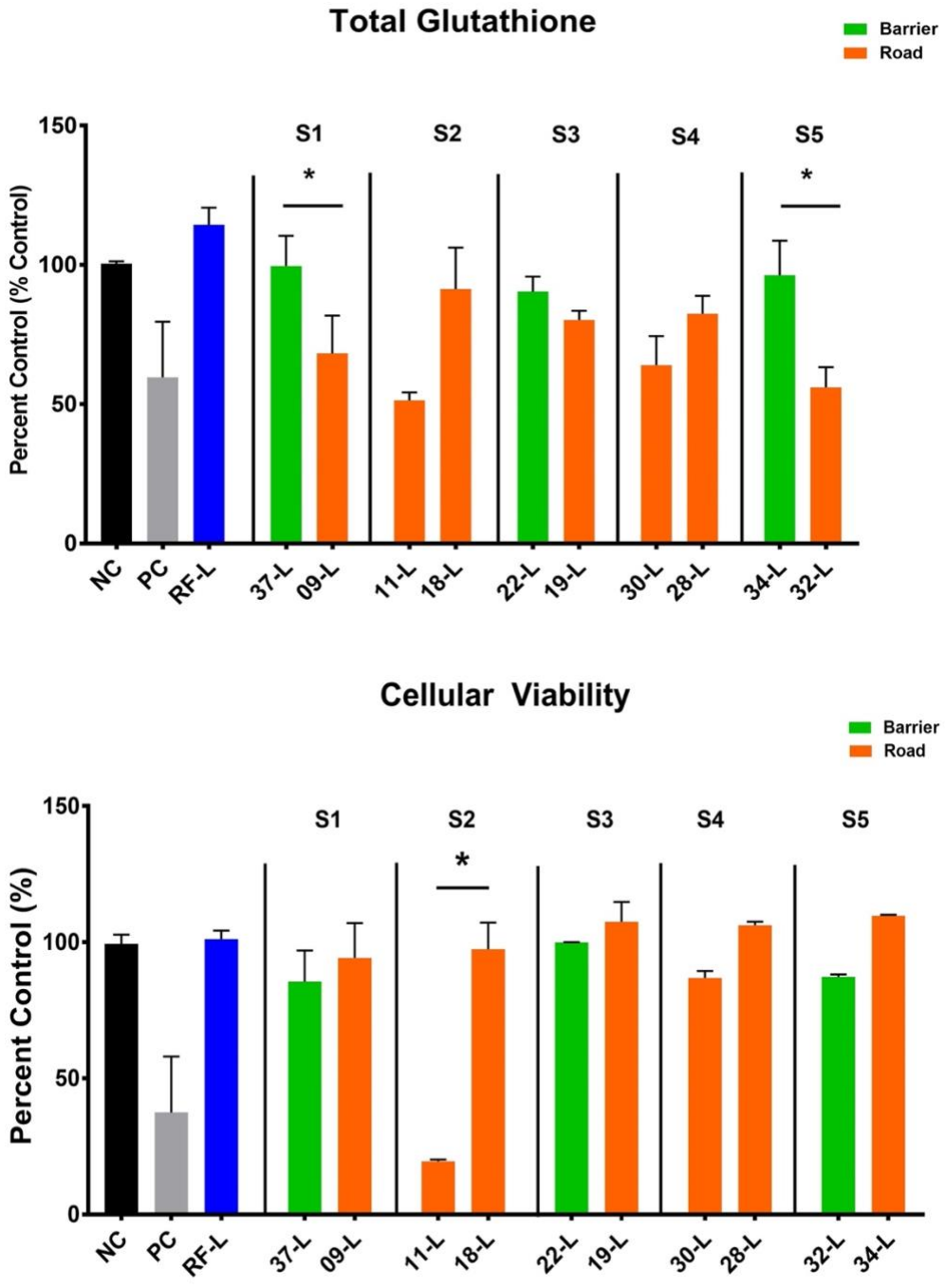

Figure 6. Modulation of Pro-Inflammatory Cytokines Due to Barrier and Road TRAP